

1           **Inconsistency in historical simulations and future projections of**  
2           **temperature and rainfall: a comparison of CMIP5 and CMIP6 models**  
3           **over Southeast Asia**

4  
5           Mohammed Magdy Hamed<sup>1,3</sup> \*, Mohamed Salem Nashwan<sup>2</sup>, Shamsuddin Shahid<sup>3</sup>,  
6           Tarmizi bin Ismail<sup>3</sup>, Xiao-jun Wang<sup>4,5</sup>, Ashraf Dewan<sup>6</sup>, Md Asaduzzaman<sup>7</sup>

7  
8           <sup>1</sup>Construction and Building Engineering Department, College of Engineering and  
9           Technology, Arab Academy for Science, Technology and Maritime Transport (AASTMT),  
10          B 2401 Smart Village, 12577, Giza, Egypt. E-mail: [eng.mohammedhamed@aast.edu](mailto:eng.mohammedhamed@aast.edu)

11          <sup>2</sup>Construction and Building Engineering Department, College of Engineering and  
12          Technology, Arab Academy for Science, Technology and Maritime Transport (AASTMT),  
13          2033 Elhorria, Cairo, Egypt. E-mail: [m.salem@aast.edu](mailto:m.salem@aast.edu)

14          <sup>3</sup>Department of Water and Environmental Engineering, School of Civil Engineering, Faculty  
15          of Engineering, Universiti Teknologi Malaysia (UTM), 81310 Skudua, Johor, Malaysia. E-  
16          mail: [sshahid@utm.my](mailto:sshahid@utm.my) (S.S.), [tarmiziismail@utm.my](mailto:tarmiziismail@utm.my) (T. I.)

17          <sup>4</sup>State Key Laboratory of Hydrology-Water Resources and Hydraulic Engineering, Nanjing  
18          Hydraulic Research Institute, Nanjing 210029, China

19          <sup>5</sup>Research Center for Climate Change, Ministry of Water Resources, Nanjing 210029, China,  
20          E-mail: [xjwang@nhri.cn](mailto:xjwang@nhri.cn)

21          <sup>6</sup>Spatial Sciences Discipline, School of Earth and Planetary Sciences, Curtin University, Kent  
22          Street, Bentley, Perth 6102, Australia, E-mail: [A.Dewan@curtin.edu.au](mailto:A.Dewan@curtin.edu.au)

23          <sup>7</sup>Department of Engineering, School of Digital, Technologies and Arts, Staffordshire  
24          University, Stoke-on-Trent, UK, E-mail: [Md.Asaduzzaman@staffs.ac.uk](mailto:Md.Asaduzzaman@staffs.ac.uk)

25  
26          \*Corresponding Author E-mail: [eng.mohammedhamed@aast.edu](mailto:eng.mohammedhamed@aast.edu)

28           **Inconsistency in historical simulations and future projections of**  
29           **temperature and rainfall: a comparison of CMIP5 and CMIP6 models**  
30           **over Southeast Asia**

31  
32   **Abstract**

33   The objective of this research was to assess the difference in historical simulations and future  
34   projections of rainfall and temperature of CMIP5 (RCP4.5 and 8.5) and CMIP6 (SSP2-4.5  
35   and 5-8.5) models over Southeast Asia (SEA). Monthly historical rainfall and temperature  
36   estimations of 13 global climate models common to both CMIPs were evaluated to assess  
37   their capability to reproduce the spatial distribution and seasonality of European Reanalysis  
38   (ERA) rainfall and temperature. Models were used to determine uncertainty with  
39   spatiotemporal variability of rainfall and temperature projections. The CMIP6 GCMs did not  
40   appear to perform better than the older CMIP5 in SEA unlike other parts of the globe, except  
41   for rainfall. The CMIP6 models showed Kling-Gupta Efficiency (KGE) values in the range  
42   of -0.48-0.6, 0.21-0.85 and 0.66-0.91 in simulating historical rainfall, maximum temperature  
43   and minimum temperature compared to 0.13-0.46, 0.3-0.86 and 0.42-0.92 for CMIP5. The  
44   improvement in CMIP6 models in SEA was in the low uncertainty in ensemble simulation.  
45   The projections of CMIP5 and CMIP6 showed a relatively smaller increase in temperature  
46   with the CMIP6 ensemble when compared to CMIP5 models, while rainfall appeared to  
47   decrease. The geographical distribution of the changes indicated a greater increase in  
48   temperature in the cooler region than in the warmer region. In contrast, there was increase in  
49   rainfall in the wetter region and a smaller improvement in the drier region. This indicates  
50   increased homogeneity in temperature spatial variability, but more heterogeneity in rainfall,  
51   in the SEA region under climate warming scenarios.

52  
53   **Keywords** Tropical climate, GCM, CMIP5/CMIP6, Uncertainty, Köppen climate  
54   classification

## 55 **1. Introduction**

56 Climate change is a global issue due to the damaging effects on various sectors, including  
57 water resources, public health, energy, and agriculture (Lee et al., 2017; Muhammad et al.,  
58 2019; Shahid, 2010; Shahid et al., 2017). Mapping possible changes in the climatic  
59 parameters is crucial for planning climate change adaptation and mitigation strategies. It is  
60 particularly important in environmentally-critical locations, where subtle changes in weather  
61 parameters may significantly impact the service sector. Global Climate Models (GCMs) have  
62 the ability to simulate the effects of greenhouse gas (GHG) emissions on climatic systems  
63 and realistically predict future conditions (Flato et al., 2013; Hartmann, 2016). These models  
64 are widely used to model past climatic conditions and project future responses to increased  
65 GHG emissions and land-use changes (Chen et al., 2014; Taylor et al., 2011; van Vuuren et  
66 al., 2011). A major advantage of GCMs is their ability to predict future climate in response  
67 to various atmospheric GHG concentration scenarios. These GCMs are available publicly as  
68 part of the Coupled Model Intercomparison Project (CMIP).

69 Most GCMs incorporate a large degree of uncertainty, primarily due to inadequate  
70 model descriptions of the physical processes driving the climate system and climate scenarios  
71 (Gao et al., 2019; Hamed et al., 2021a; Weigel et al., 2010). Certain models, however, are  
72 capable of resolving regional climatic events, thereby increasing their usefulness in  
73 predicting future climate change scenarios for a given region. It is normally a good idea to  
74 utilize all available climate models to reflect a complete range of future changes. CMIP  
75 models have rigorously improved over the years to overcome these uncertainties, from  
76 CMIP1 to the latest version, CMIP6 (Eyring et al., 2016).

77 CMIP6 GCMs differ from previous CMIPs in that the newest version provides a more  
78 accurate depiction of the Earth's physical processes. Additionally, the CMIP6 model forecasts  
79 additional scenarios using shared socioeconomic pathways (SSPs) (O'Neill et al., 2014;  
80 Schlund et al., 2020). These updated climate projections take socioeconomic developments,  
81 technological advancement, and other environmental factors (such as land use) into account  
82 (Moss et al., 2010), enabling the development of new scenarios to better evaluate the  
83 consequences of climate change policies. CMIP6 places a premium on coordinated  
84 experiments to gain a better understanding of the processes behind climate variability. As a  
85 result, CMIP6 GCMs are expected to minimize possible bias to a greater extent than their  
86 predecessors (Arias et al., 2021; Iqbal et al., 2021; Song et al., 2021b).

87 Southeast Asia (SEA), located between two oceans (the Pacific to the east and the  
88 Indian to the west) and two continental regions (Asia and Australia), is considered the largest

89 archipelago in the world (Chang et al., 2005). The climate in this region is tropical, with high  
90 temperatures and well-distributed monthly rainfall of >200 mm. The climate is determined  
91 by latent heat release near the equator and convective tropical air masses. The rainfall  
92 distribution is controlled by a land-sea breeze process, resulting from the interaction of  
93 elevated island topography and synoptic winds (Hamed et al., 2021b; Qian, 2008).

94 SEA has experienced different climatic extremes over the last 50 years (including  
95 droughts during El Nino events and heavy rains in La Nina periods) especially in the  
96 Indonesian region (Dewi, 2010; Nasional, 2012). The mean temperature has risen by 0.1-  
97 0.03°C per decade over the past 50 years, and the sea level has risen by 1-3 mm per year  
98 (IPCC, 2007). The severity and frequency of climatic extremes are likely to increase, putting  
99 the SEA region at risk of climate change impacts (Thirumalai et al., 2017; Ge et al., 2019;  
100 Nashwan et al., 2018a; Raghavan et al., 2017). Significant changes in seasonal rainfall  
101 patterns and an increase in the frequency of flooding and water shortage would profoundly  
102 affect many service sectors (Nashwan et al., 2018b; Nashwan and Shahid, 2022; Ziarh et al.,  
103 2021). In order to be prepared for these increased impacts, policymakers must be informed  
104 about the climate change implications for these areas and the adaptation methods required to  
105 mitigate impacts and increase industry resilience.

106 Numerous studies have examined both the historical and potential future climate  
107 change in SEA and adjacent areas using GCMs (Desmet and Ngo-Duc, 2021; Iqbal et al.,  
108 2021; Kang et al., 2019; Khadka et al., 2021; McSweeney et al., 2015; Noor et al., 2019;  
109 Salman et al., 2020; Supari et al., 2020; Supharatid et al., 2021; Tangang et al., 2020). For  
110 example, Iqbal et al. (2021) used compromised programming to rank 35 CMIP6 GCMs for  
111 Mainland Southeast Asia (MSEA). Analysis revealed that three GCMs could accurately  
112 reproduce annual mean rainfall over central and southern regions. Desmet and Ngo-Duc,  
113 (2021) investigated rainfall, near-surface temperature and wind for 28 CMIP6 models in  
114 SEA. They ranked GCMs by combining two different scores (spatial and temporal) to  
115 generate each variable score. A final global score, combining all variables, is then reported.  
116 Khadka et al. (2021) compared 28 CMIP5 and 32 CMIP6 GCMs to assess their ability to  
117 replicate large-scale atmospheric circulations over the SEA summer monsoon domain. These  
118 showed better performance for the CMIP6 GCMs than for CMIP5. These studies evaluated  
119 the historical performance of GCMs in regards of simulating climate over SEA. Only  
120 Supharatid et al. (2021) investigated the change in rainfall and temperature in SEA using  
121 CMIP6, although their study was confined to MSEA. They utilized two SSP scenarios to  
122 examine changes in climate parameters. It appears that a comprehensive assessment

123 involving a comparison of CMIP5 and CMIP6 historical simulations and future projection  
124 over the entire SEA (comprising both mainland and maritime continents) is lacking. Despite  
125 the governments in this region having already taken steps to reduce climate change effects  
126 based on the CMIP5 modelling, this planning could be negatively impacted by population  
127 growth and large-scale economic development. So the risk associated with climate change  
128 would not be uniform over the whole region. Governments in the region need current,  
129 detailed information to inform the adaptation strategies selected for various SSPs. A  
130 comparative evaluation of the projections, based on CMIP5 and CMIP6 models, is essential  
131 for the region in order to streamline all existing adaptation measures.

132 This study aims to evaluate the difference in previous historical estimations and  
133 projections of CMIP5 and CMIP6 models over Southeast Asia. Both rainfall and temperature  
134 data are examined and evaluated to assess the validity of the decision-making process based  
135 on the various projections.

136

## 137 **2. Description of the study area and data**

### 138 **2.1. Southeast Asia (SEA)**

139 SEA lies between latitude  $-10^{\circ}$  -  $30^{\circ}$ N and longitude  $90^{\circ}$  -  $141^{\circ}$ E (Figure 1). SEA covers an  
140 area of about 4,550,000 km<sup>2</sup>. It includes eleven countries and is made up of two main regions  
141 (Mainland and Maritime Southeast Asia). SEA is located within the zone of the Asian  
142 monsoon cycle, located between the Pacific and Indian Oceans. It is one of Asia's most active  
143 regions affected by convective heating processes. SEA has a generally level topography apart  
144 from some parts of Myanmar and Indonesia, where the elevation rises to 4000 m above sea  
145 level. The average yearly rainfall for the region varies between 750 and 5000 mm (Khan et  
146 al., 2019; Peel et al., 2007; Yang et al., 2021), and the mean temperature is 25 °C. As a result  
147 of the diverse spatiotemporal atmospheric processes occurring within the region, climate  
148 extremes such as droughts and floods are common in most parts of SEA.

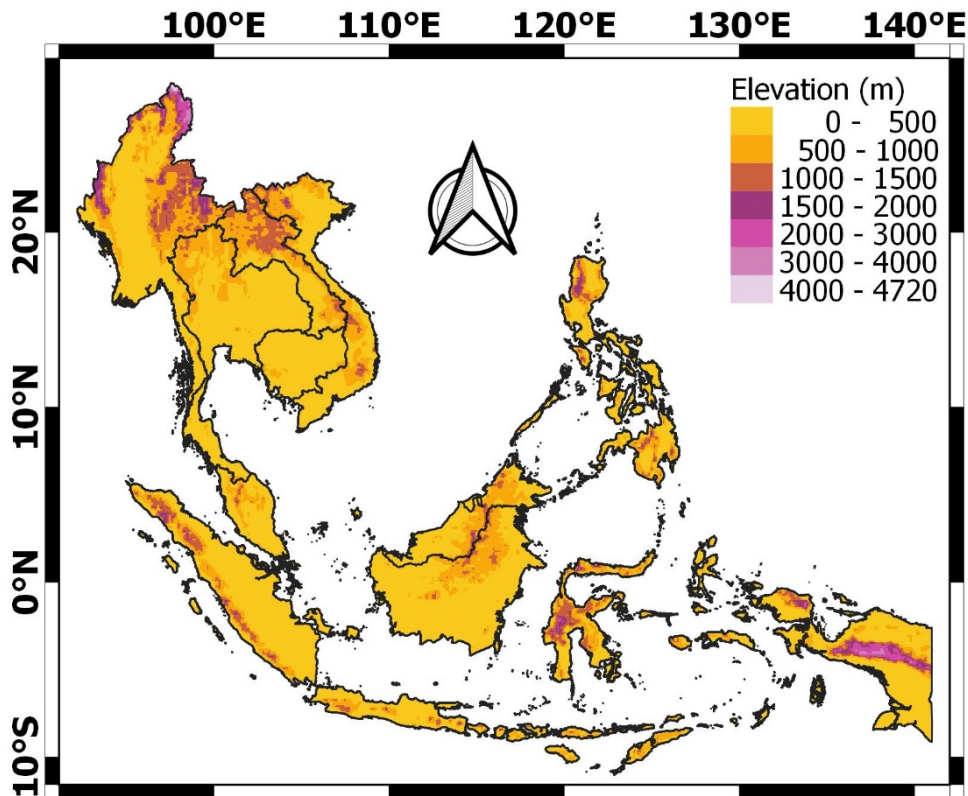


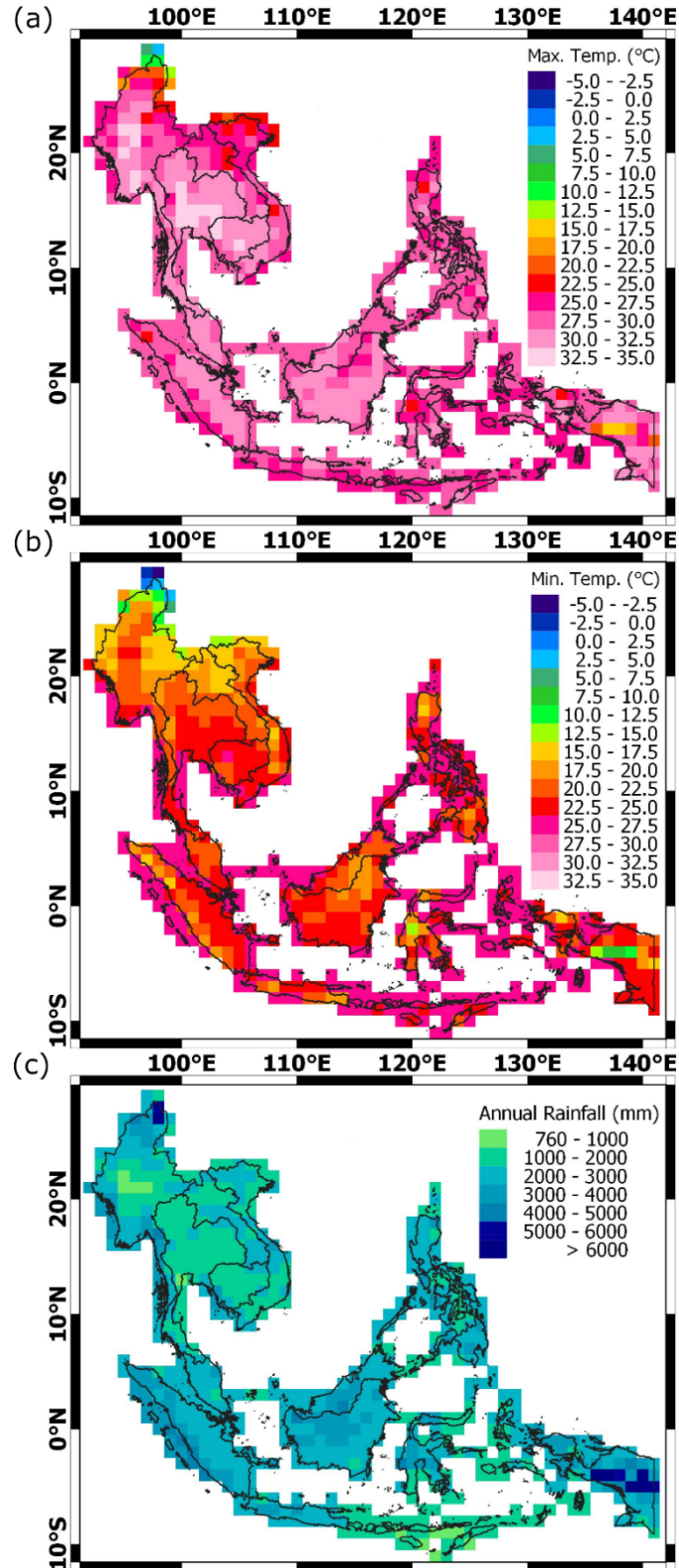
Figure 1 Southeast Asian topography

## 2.2. Gridded rainfall and temperature dataset

To assess the ability of the GCMs' to simulate annual rainfall, and maximum and minimum temperatures, ERA5 - a global high-resolution reanalysis dataset, is used. ERA5 is the fifth edition of the Copernicus Climate Change Service's (C3S) atmospheric, oceanic, and land-surface reanalysis product of the European Centre for Medium-Range Weather Forecasts (ECMWF) (Hersbach et al., 2020). This provides data on 240 atmospheric variables for different pressure level settings. ERA5 is generated by combining an enhanced version of the Integrated Forecasting System (IFS) cycle 41r2 with high-quality global observations. This study used the hourly ERA5 dataset of two climatic variables (e.g., rainfall and near-surface temperature) with a 0.25-degree spatial resolution, spanning the period from January 1979 to December 2005. The hourly rainfall is used to estimate the total monthly rainfall, while the highest and lowest diurnal temperatures were used to extract the average maximum and minimum temperatures. SEA is considered a data-scarce region due to the unavailability of high-quality long-term observation data (Li, 2020). The evenly spaced gridded dataset is generally used for model validation in data-scarce regions. ERA5 is a reanalysis climate data product that provides consistent high-resolution hourly data of several

167 climate variables. It should be noted that several studies have reported the use of ERA5 as a  
168 reference dataset near SEA (Khadka et al., 2021; Zhai et al., 2020; Zuluaga et al., 2021).

169 The spatial distribution of mean annual rainfall,  $T_{mx}$ , and  $T_{mn}$  over SEA is shown in  
170 Figure 2. Hkakabo Razi Mountains in the north and Papua in the south experience the  
171 highest annual rainfall (>5000 mm), while the lowest can be found in the middle of Myanmar.  
172  $T_{mx}$  is homogeneous in SEA except for the high mountainous regions.  $T_{mn}$  ranges from 15 to  
173 30 °C over SEA. However,  $T_{mn}$  in the northern region of SEA can be as low as -5 °C.

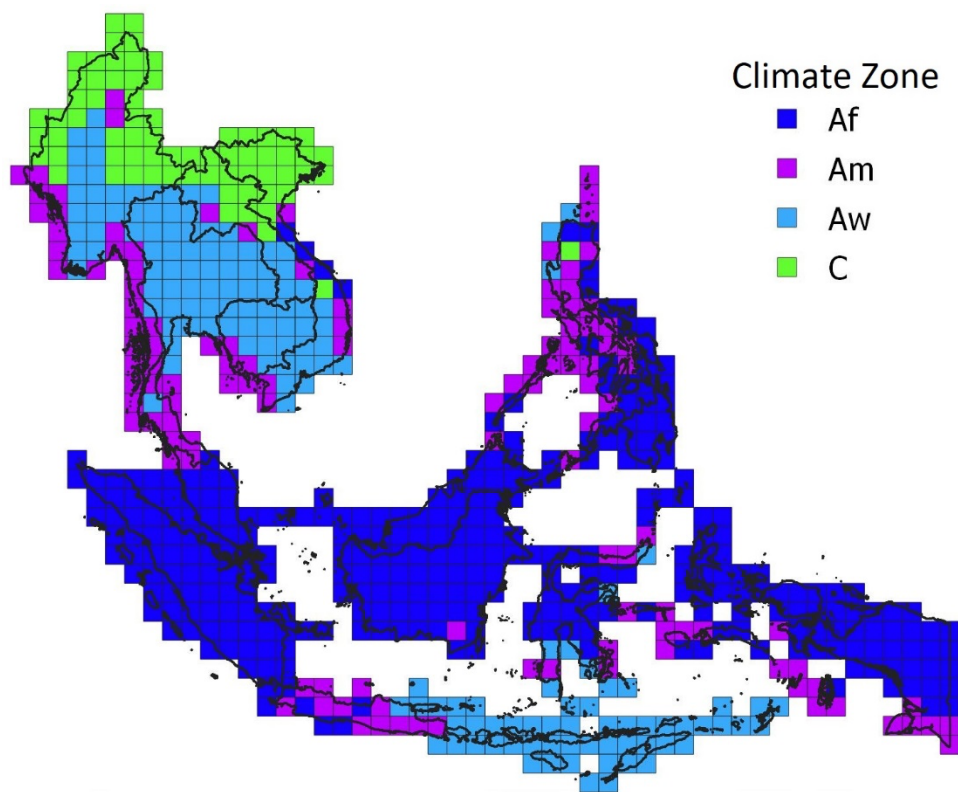


174  
 175 Figure 2 Spatial variability of yearly mean (a)  $T_{mx}$  and (b)  $T_{mn}$ , and (c) annual total rainfall  
 176 over SEA during 1979–2005, estimated via ERA5.

177 SEA is subject to a wide variability in climatic conditions. The region is classified  
 178 into six climate zones based on Köppen climate classification (Peel et al., 2007): tropical

179 rainforest climate (Af), tropical monsoon climate (Am), tropical Savannah climate (Aw),  
180 temperate without dry season (Cf), temperature dry summer (Cs), and temperature dry winter  
181 (Cw). Due to small areal coverage of Cf, Cs, and Cw, they are combined and included in  
182 zone C (Figure 3). Af is major climate zone over the SEA, covering 47% of total area,  
183 whereby annual rainfall varies from 2000 to 4000 mm. During winter, the temperature drops  
184 to near freezing point (-5 to 0 °C), particularly in zone C, however it often rises to above 35  
185 °C during some summer days, particularly in Thailand in the Aw zone. Annual rainfall ranges  
186 from 760 to 1000 mm in most of the Aw zone. In general, the temperature in both Af and  
187 Am zones is greater than 18 °C, however the total rainfall amounts received are different  
188 (Alvares et al., 2013).

189



190

191 Figure 3 Köppen climate classification of SEA based on ERA5 (1979-2005). Köppen climate  
192 classes are Tropical rainforest climate (Af), Tropical monsoon climate (Am), Tropical  
193 Savannah climate (Aw), Temperate without dry season (Cf), Temperature dry summer (Cs),  
194 and Temperature dry winter (Cw).

195

### 196 2.3. Global climate models (GCMs)

197 This study assesses the performance of 13 CMIP5 GCM's (Taylor et al., 2012) and their  
198 updated versions, CMIP6 (Eyring et al., 2016) over SEA. The output of the models have been

199 downloaded from the open-access platform <https://esgf-node.llnl.gov>. This site provides  
 200 historical and future projections of monthly rainfall, Tmx and Tmn. The models details are  
 201 presented in Table 1. Out of several variant labels available, the first one, r1i1p1 for CMIP5  
 202 and r1i1p1f1 for CMIP6, is chosen to simplify the evaluation process. CMIP5 investigates  
 203 several greenhouse gas emissions scenarios through the radiative concentration pathways  
 204 (RCPs). In CMIP6, new SSPs are used which consider possible changes in the Earth's  
 205 environment, as well as global economic and demographic trends. Future projections of the  
 206 RCP 4.5 and 8.5 of CMIP5 are compared with their equivalent radiative forcing in CMIP6,  
 207 SSP2-4.5 and SSP5-8.5 in this study.

208 Table 1 Detailed description of the CMIP5 and CMIP6 GCMs used in this research

<b>Institution / Country</b>	<b>Abbreviation</b>	<b>Model</b>	<b>Resolution</b>
Australian Research Council Centre of Excellence for Climate System Science, Australia	ACCESS	CMIP 5 ACCESS1-3	$1.90 \times 1.20^\circ$
		CMIP 6 ACCESS-CM2	$1.87 \times 1.25^\circ$
Beijing Climate Center, Beijing, China	BCC	CMIP 5 BCC-CSM1.1-M	$2.80 \times 2.80^\circ$
		CMIP 6 BCC-CSM2-MR	$1.12 \times 1.12^\circ$
Canadian Centre for Climate Modelling and Analysis, Victoria, Canada	CANESM	CMIP 5 CANESM2	$2.80 \times 2.80^\circ$
		CMIP 6 CanESM5	$2.79 \times 2.81^\circ$
Euro-Mediterranean Centre on Climate Change coupled climate model, Italy	CMCC	CMIP 5 CMCC-CM	$0.70 \times 0.70^\circ$
		CMIP 6 CMCC-ESM2	$0.94 \times 1.25^\circ$
EC-Earth Consortium, Europe	EC-EARTH	CMIP 5 EC-EARTH	$1.10 \times 1.10^\circ$
		CMIP 6 EC-Earth3	$0.35 \times 0.35^\circ$
Chinese Academy of Sciences Flexible Global Ocean-Atmosphere-Land System model, China	FGOALS	CMIP 5 FGOALS-g2	$2.80 \times 2.08^\circ$
		CMIP 6 FGOALS-g3	$2.00 \times 2.00^\circ$
Geophysical Fluid Dynamics Laboratory, NJ, USA	GFDL-ESM	CMIP 5 GFDL-ESM2G	$2.50 \times 2.00^\circ$
		CMIP 6 GFDL-ESM4	$1.00 \times 1.25^\circ$
Institute for Numerical Mathematics, Russia	INMCM	CMIP 5 INMCM4.0	$2.00 \times 1.50^\circ$
		CMIP 6 INM-CM5-0	$2.00 \times 1.50^\circ$
Institute Pierre Simon Laplace (IPSL), Paris, France	IPSL-CM-LR	CMIP 5 IPSL-CM5A-LR	$3.70 \times 1.90^\circ$
		CMIP 6 IPSL-CM6A-LR	$2.50 \times 1.27^\circ$
Japan Agency for Marine-Earth Science and Technology (JAMSTEC), Kanagawa, Japan	MIROC	CMIP 5 MIROC5	$1.40 \times 1.40^\circ$
		CMIP 6 MIROC6	$1.40 \times 1.40^\circ$
		CMIP 5 MPI-ESM-MR	$1.90 \times 1.90^\circ$

<b>Institution / Country</b>	<b>Abbreviation</b>	<b>Model</b>		<b>Resolution</b>
Max Planck Institute for Meteorology (MPI-M), Germany	MPI-ESM-HR	CMIP 6	MPI-ESM1-2-HR	$0.94 \times 0.94^\circ$
	MPI-ESM-LR	CMIP 5	MPI-ESM-LR	$1.90 \times 1.90^\circ$
		CMIP 6	MPI-ESM1-2-LR	$1.87 \times 1.86^\circ$
Meteorological Research Institute, Ibaraki, Japan	MRI	CMIP 5	MRI-CGCM3	$1.10 \times 1.10^\circ$
		CMIP 6	MRI-ESM2-0	$1.12 \times 1.12^\circ$

209

### 210 **3. Methodology**

211 ERA5  $0.25^\circ \times 0.25^\circ$  reanalysis dataset is used as a reference to evaluate CMIP5 and CMIP6  
212 GCMs. The evaluation process entails examining past performance of the three climatic  
213 variables (e.g., mean annual rainfall,  $T_{mx}$  and  $T_{mn}$ ). This is carried out using statistical and  
214 graphical metrics. Ultimately the model ensemble mean is used to project future changes for  
215 each climate zone of SEA for different CMIPs. GCMs have spatial resolution ranges from  
216  $0.70^\circ$  to  $3.70^\circ$  (Table 1), so they are normally interpolated to a common spatial resolution of  
217  $1.0^\circ \times 1.0^\circ$  using bilinear interpolation technique. The ERA5 data is also aggregated to the  
218 resolution of  $1.0^\circ \times 1.0^\circ$ , so all datasets have similar grid sizes and therefore provide an  
219 unbiased comparison. Methodological details are presented below.

#### 220 **3.1. Statistical and graphical analyses**

221 The Kling-Gupta efficiency (KGE) is employed to estimate the relative performance of the  
222 two CMIPs (Gupta et al., 2009; Kling et al., 2012). The KGE is a single metric designed to  
223 evaluate three statistical characteristics together (e.g., Pearson's correlation ( $r$ ), spatial  
224 variability ratio and the normalized variance) as shown in equation (1). The combination of  
225 three metrics provides valuable diagnostic information about the model's performance. KGE  
226 is less susceptible to extremes and has greater capability to describe and quantify the overall  
227 fitness of GCMs (Radcliffe and Mukundan, 2017). The KGE value varies between 1 and  $-\infty$ ,  
228 where 1 represents a complete match. There is no specific meaning attached to the KGE value  
229 when it equals zero. However, Knoben et al., (2019) compared the KGE with the Nash-  
230 Sutcliff efficiency index and noted that KGE values above -0.41 represented a reasonable  
231 performance, while values closer to 1 generally indicated high performance. The KGE is  
232 calculated for three climate variables of each GCM compared to the reference dataset (1979-  
233 2005).

$$KGE = 1 - \sqrt{(r - 1)^2 + \left(\frac{\mu_{GCM}}{\mu_{ref}} - 1\right)^2 + \left(\frac{\sigma_{GCM}/\mu_{GCM}}{\sigma_{ref}/\mu_{ref}} - 1\right)^2} \quad (1)$$

234 where  $\mu_{GCM}$  and  $\mu_{ref}$  are the mean, and  $\sigma_{GCM}$  and  $\sigma_{ref}$  are the standard deviation for GCM  
235 and ERA5 data, respectively.

236 The Taylor diagram (Taylor, 2001) is employed to visually represent the performance  
237 of each GCM. The diagram is a robust graphical plot that integrates three statistical metrics,  
238 degree of correlation (R), centered root-mean-square error (CRMSE) and ratio of spatial  
239 standard deviation (SD). CRMSE determines the discrepancies between two CMIPs and the  
240 ERA5 observed data. The blue line in the diagram represents constant CRMSD values, with  
241 values increasing with distance from the center.

242 Statistical tests were employed to estimate the similarity between the seasonal  
243 variability of CMIPs and ERA5 rainfall,  $T_{mx}$  and  $T_{mn}$ , following Baker and Huang (2014).  
244 The tests include 1) t-test to show the similarity in the mean, 2) F-test to assess the similarity  
245 in data variance, and 3) Kolmogorov–Smirnov (KS) test to evaluate the similarity in data  
246 distribution (Sardeshmukh et al., 2000).

### 247 **3.2. Future projections**

248 Future projections of annual rainfall,  $T_{mx}$  and  $T_{mn}$  using GCMs of two CMIPs are compared  
249 with the historical period (1979-2005) to evaluate possible future climate changes in SEA.  
250 Two projections are considered: the medium (RCP4.5 and SSP2-4.5) and high (RCP8.5 and  
251 SSP5-8.5) impact scenarios. For a detailed comparison, future horizon was divided into near  
252 (2020-2059) and far (2060-2099) futures. The median and 95% confidence band of the  
253 projection interval are considered for each scenario in order to quantify the associated  
254 uncertainty of the different CMIP models. The seasonal variability of different climate zones  
255 for rainfall,  $T_{mx}$  and  $T_{mn}$  are measured for each model. Finally, maps are prepared to depict  
256 percentage of change in rainfall and absolute change in temperatures (°C).

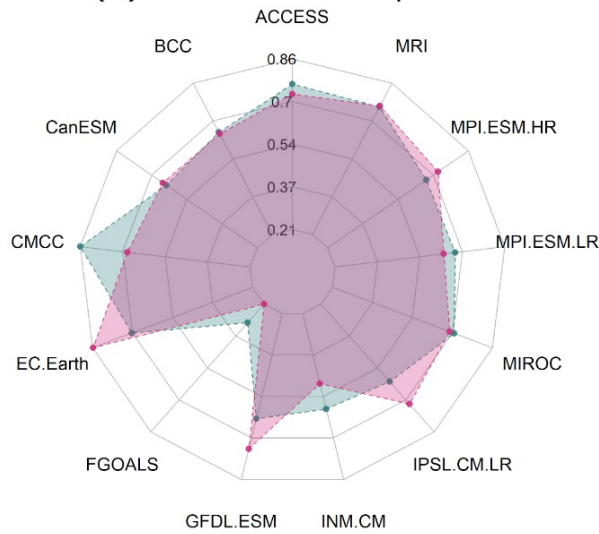
## 257 **4. Results**

### 258 **4.1. Evaluating skills of CMIP5 and CMIP6 GCMs**

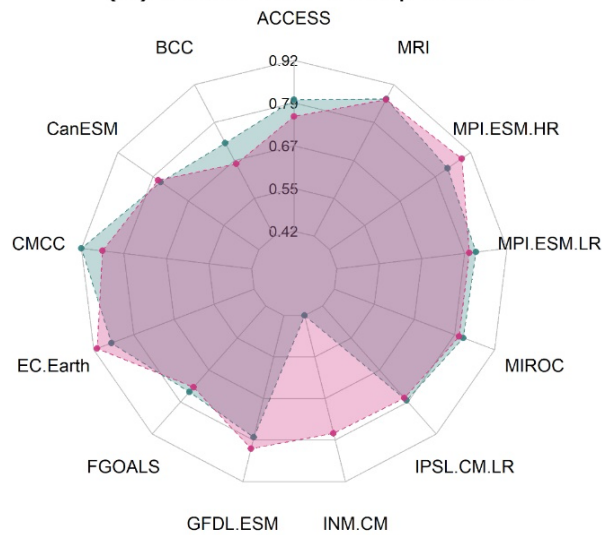
259 Figure 4 depicts the ability of two CMIPs to replicate annual rainfall,  $T_{mx}$ , and  $T_{mn}$  in terms  
260 of KGE. A single radar chart is used to present KGE of CMIP5 (in light green) and CMIP6  
261 (in light red) GCMs for each climate variable. KGE values less than zero on the rainfall radar

262 chart are defined as zero for illustration purposes. It shows that GCMs are able to estimate  
263  $T_{mn}$  better than  $T_{mx}$  and rainfall in SEA. The performance of the CMIP5 models and their  
264 improvements in CMIP6 are almost the same in simulating  $T_{mx}$  and  $T_{mn}$ . Few models of  
265 CMIP6 simulated  $T_{mx}$  better than previous versions, namely: MPI-ESM-HR, IPSL-CM-LR,  
266 GFDL-ESM, EC-Earth, CanESM and MRI. Both versions of FGOALS simulated a lower  
267 value of  $T_{mx}$  than other models, indicating poor modelling capability. For  $T_{mn}$ , only five  
268 models of CMIP6 indicated better performance than their predecessors, including MPI-ESM-  
269 HR, INM-CM, GFDL-ESM, EC-Earth and CanESM. INM-CM showed the largest  
270 improvement in CMIP6 for  $T_{mn}$ . Although the performance of the models of both CMIPs was  
271 nearly identical in replicating historical temperatures, CMIP6 GCMs displayed an enhanced  
272 ability to simulate historical rainfall in all cases apart from FGOALS and IPSL-CM-LR.  
273 Among the CMIP6 models, EC-EARTH was best in replicating all variables. ACCESS of  
274 CMIP6 exhibited the best performance in replicating rainfall (KGE 0.59) and CMCC of  
275 CMIP5 in replicating  $T_{mx}$  and  $T_{mn}$  (KGEs 0.86 and 0.92, respectively). KGEs of both  
276 FGOALS and IPSL-CM-LR were poor (KGEs -0.31 and -0.48, respectively) for rainfall,  
277 therefore indicating poor capability.

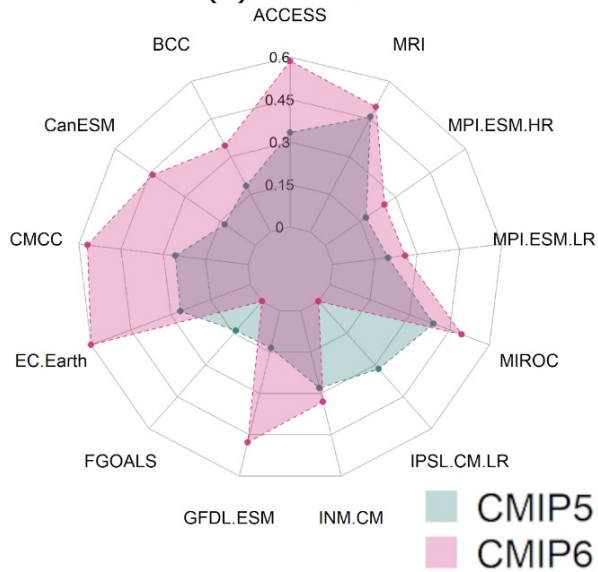
(a) Maximum Temperature



(b) Minimum Temperature



(c) Rainfall



CMIP5  
CMIP6

278

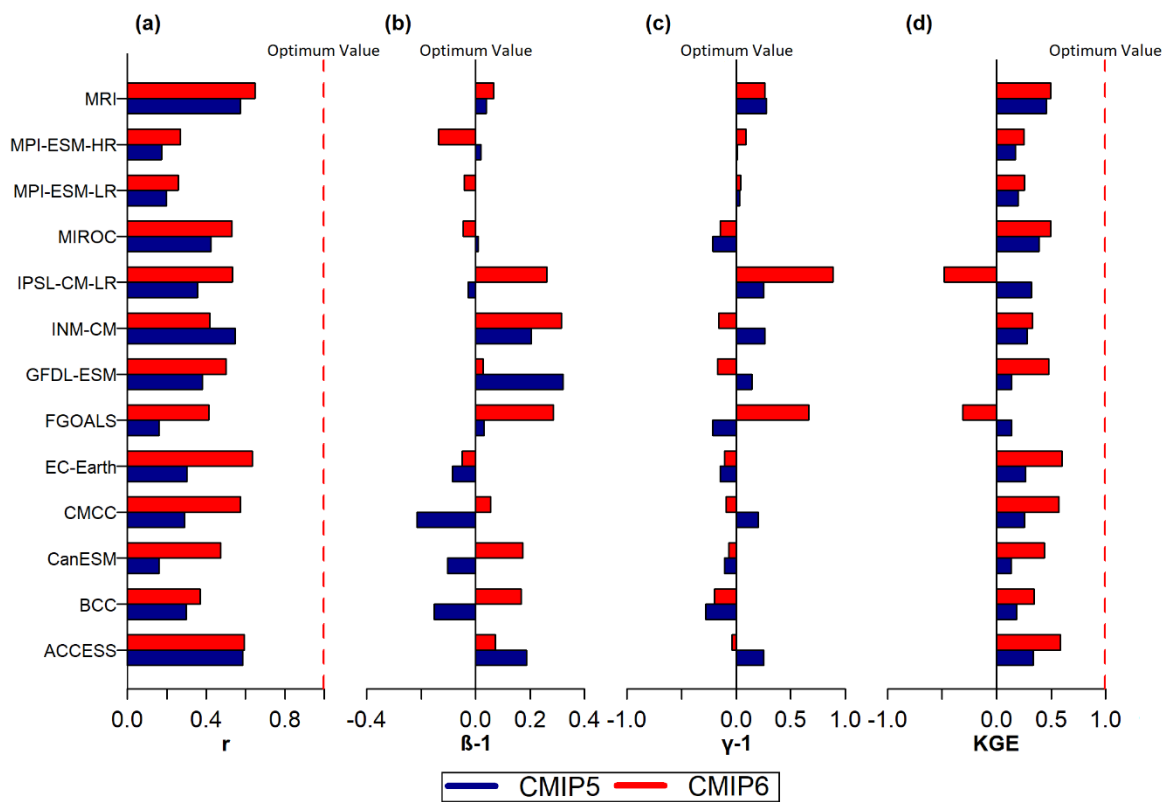
279

280

Figure 4 Performance of CMIP5 and CMIP6 GCMs in estimating historical annual average: (a)  $T_{mx}$ , (b)  $T_{mn}$ ; and (c) rainfall during 1979-2005

281 KGE is the integration of three statistical metrics, namely Pearson's correlation ( $r$ ),  
 282 mean of GCM to mean of ERA5 ( $\beta$ ) and variability ratio ( $\gamma$ ). Figure 5 presents the three  
 283 components of KGE in terms of  $r$ ,  $\beta-1$  and  $\gamma-1$  aiming to illustrate the most influencer  
 284 component of the final KGE score. The  $r$ ,  $\beta$ ,  $\gamma$  and KGE of CMIP5 and CMIP6 GCMs in  
 285 simulating historical rainfall are presented in blue and red bars. The result indicates that all  
 286 the components contribute significantly to a higher value of KGE. However, models that  
 287 have near optimum values of  $\beta$  and  $\gamma$  (e.g., MPI-ESM-LR) showed a low KGE due to low  $r$ ,  
 288 indicating a bit higher influence of spatial correlation on model performance.

289



290

291 Figure 5 Bar charts show the performance of CMIP5 and CMIP6 in simulating historical  
 292 rainfall based on KGE and its components.

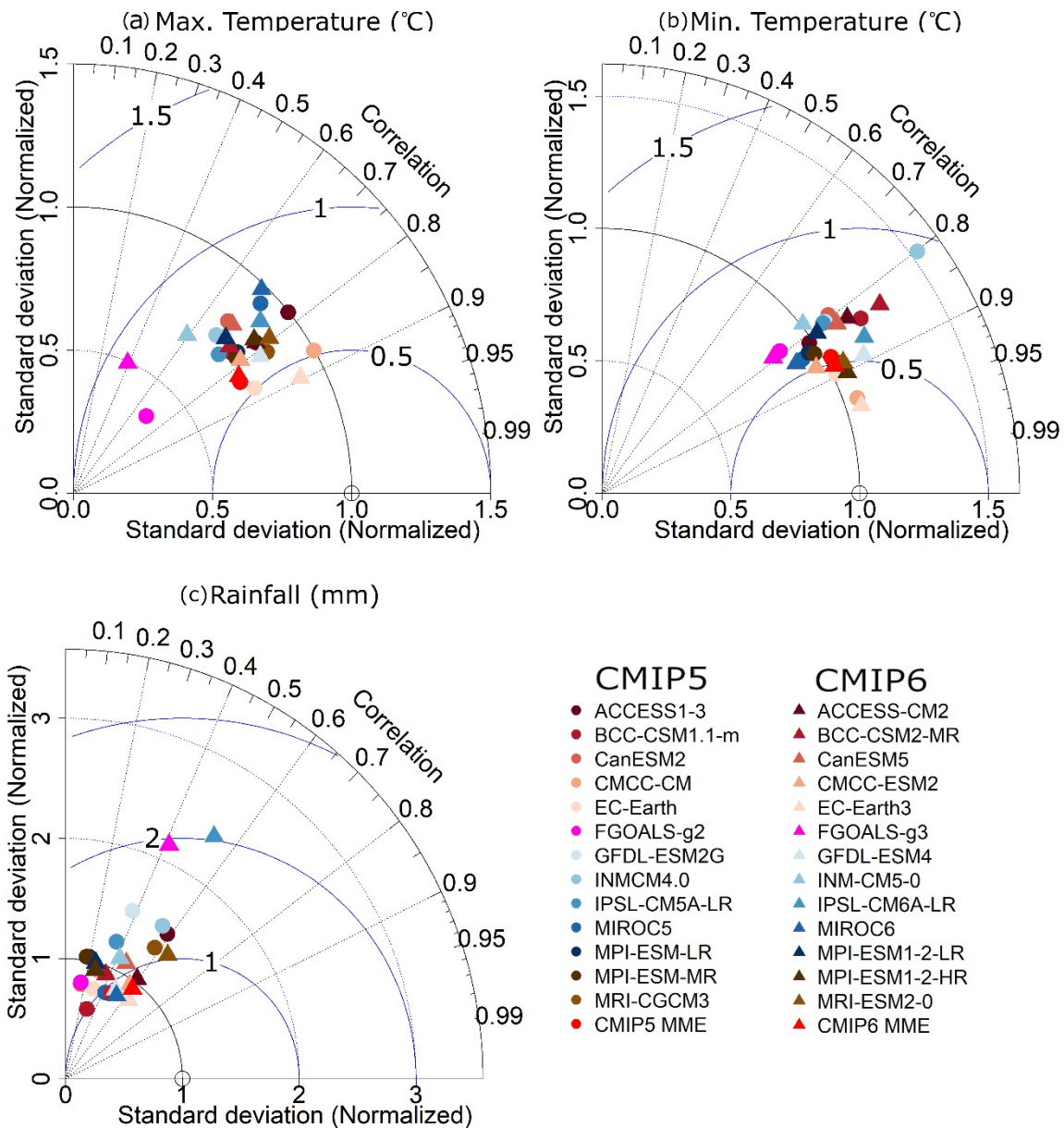
293

#### 294 4.2. Taylor diagram

295 The ability of the two CMIP models to estimate annual rainfall,  $T_{mx}$  and  $T_{mn}$  are presented  
 296 (along with their MME means) as Taylor diagrams (Figure 6). Hollow circle on the x-axis  
 297 presents reference data (i.e., ERA5). The CMIP5 and CMIP6 models are represented using  
 298 coloured circles and triangles, respectively. The model symbol nearest to the hollow circle  
 299 indicates the best performing model. The correlation of the models with the reference data is

300 best for  $T_{mn}$  (0.85). This is followed by  $T_{mx}$  (0.75) and then rainfall (0.45). A strong  
 301 correlation for  $T_{mn}$  indicates better capability of GCMs of both CMIPs in modeling  $T_{mn}$ .  
 302 Model over and underestimation, however, is noted. FGOALS of both CMIPs  
 303 underestimated  $T_{mx}$  and  $T_{mn}$  variability, while INM-CM5-0 overestimated  $T_{mn}$  variability.  
 304 The majority of models, of both CMIPs, simulated observed rainfall variability reasonably  
 305 well, except for a large overestimation by IPSL-CM6A-LR and FGOALS-g3.

306



307  
 308 Figure 6 Taylor diagrams, showing skill of the GCMs of two CMIPs in simulating: (a)  $T_{mx}$ ;  
 309 (b)  $T_{mn}$ ; and (c) rainfall

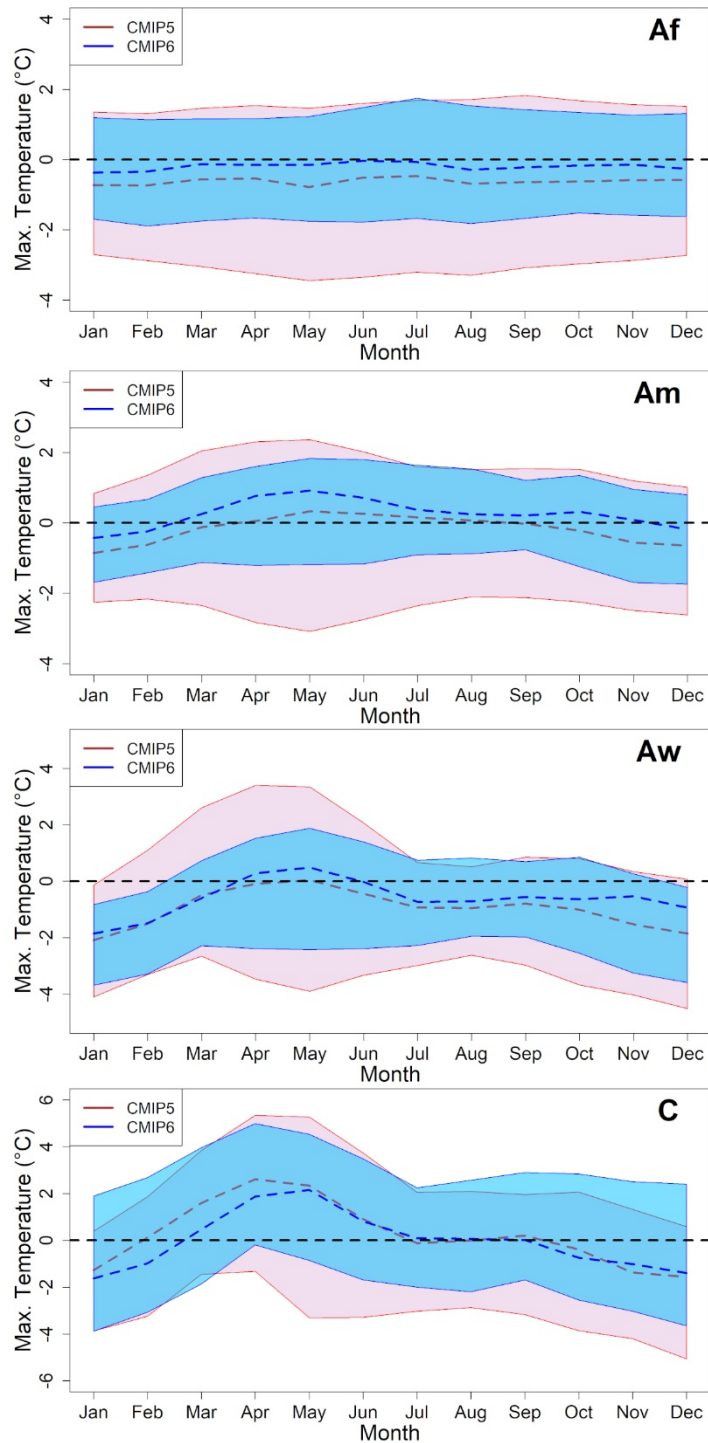
310

311

312 **4.3. Seasonal variability**

313 The multimodel ensemble (MME) medians of the available 13 GCMs for both CMIPs have  
314 been used to show bias in the seasonal variability of temperature and rainfall for each climatic  
315 zone when compared to ERA5. Figure 7 shows the month-to-month bias in  $T_{mx}$ . This is  
316 estimated by subtracting the CMIPs MME from ERA5. The dashed red line represents the  
317 bias in the CMIP5 MME median, while the dashed blue line represents the bias in the CMIP6  
318 MME median. The horizontal black dashed line represents the zero bias. The 95% confidence  
319 interval band of GCMs' bias has also been provided to show simulation uncertainty.

320 Overall, the bias in MME median of CMIP6 was more aligned to the zero line than  
321 CMIP5. The 95% confidence interval band of the CMIP6 ensemble was also thinner,  
322 suggesting lower uncertainty in their estimates of  $T_{mx}$  than for CMIP5. The results also  
323 indicated that the inner model differences of CMIP6 were far less than for CMIP5. Both  
324 versions of CMIPs displayed higher uncertainties in simulating seasonal variability of  $T_{mx}$  in  
325 climate zone C than in other zones. Both CMIPs underestimated  $T_{mx}$  in zone Af. CMIP6  
326 overestimated  $T_{mx}$  in Am for all months, except January and February. Both versions also  
327 underestimated  $T_{mx}$  in the Aw climate zone for all months, except for the April to June period.



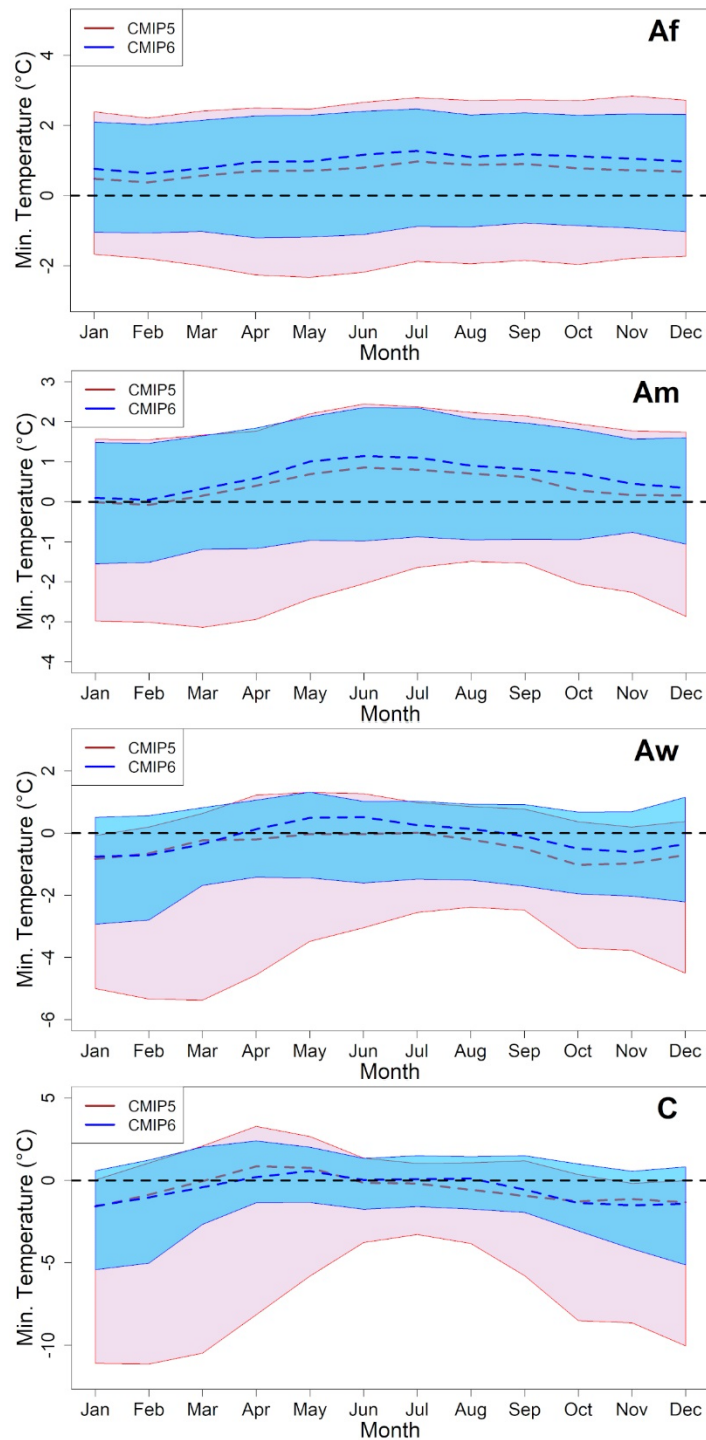
328

329 Figure 7 Seasonal variability in mean bias in  $T_{mx}$  of CMIP5 and CMIP6 GCMs compared  
 330 to ERA5 dataset for four different climate zones (AF, Am, Aw and C) of SEA

331

332 Figure 8 presents the month-to-month variability of bias in  $T_{mn}$ , estimated by the two  
 333 CMIPs. Like  $T_{mx}$ , CMIP5 shows larger inter-modality in  $T_{mn}$  than CMIP6. This indicates low  
 334 uncertainty in the CMIP6 simulations when compared to CMIP5. For most months, a subtle  
 335 overestimation by GCMs of both CMIPs was noticed for the Af and Am zones, especially by

336 CMIP6. The median bias for the MMEs was nearly identical with ERA5 for the climate zone  
 337 C, while the bias confidence interval band of CMIP5 was between -11 and 4 °C.

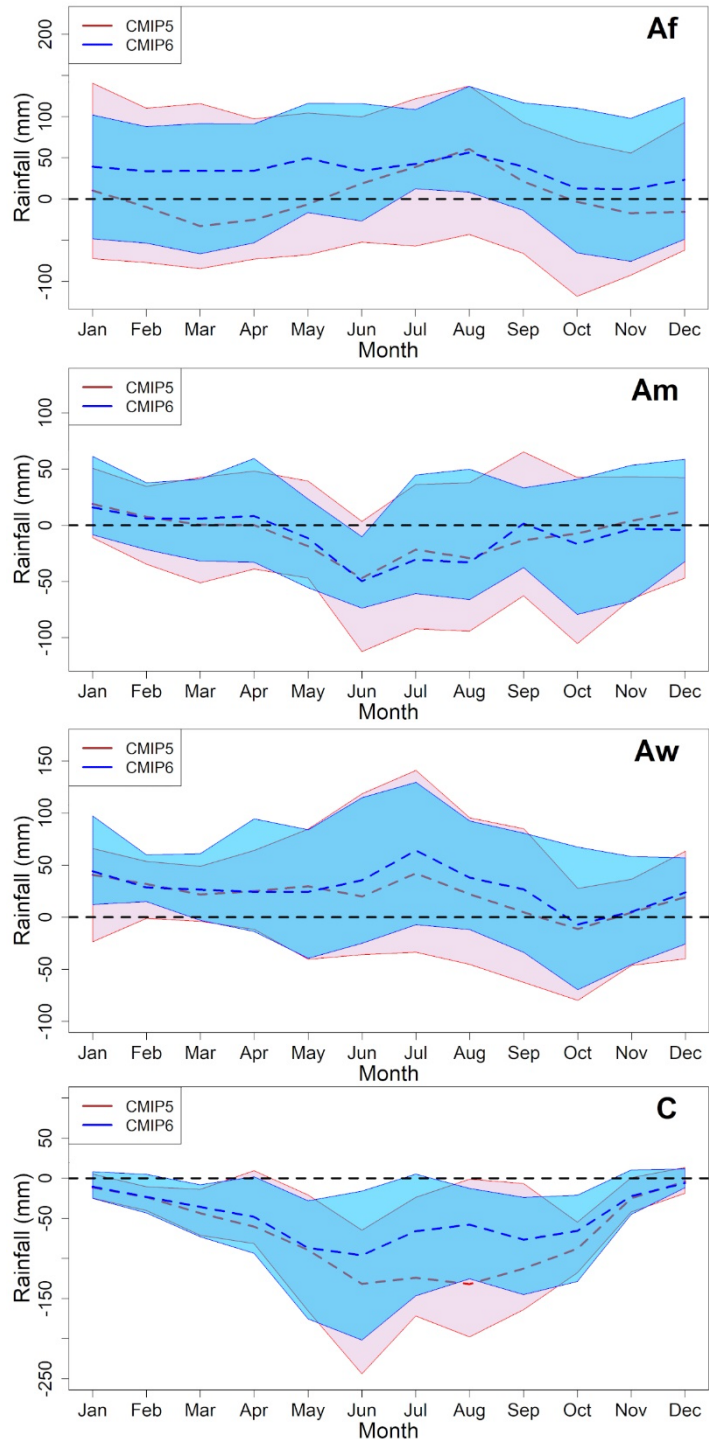


338  
 339

Figure 8 Same as Figure 7, but for Tmn

340 Similar results are seen for rainfall. Uncertainty in the CMIP6 rainfall bias (Figure 9)  
 341 band is thinner than CMIP5 bias for all climate zones. However, CMIP6 MME overestimated  
 342 rainfall for the Af zone to a greater degree than for CMIP5 MME. In the Am and Aw zone,  
 343 MME of both CMIPs under and overestimated monsoon rainfall, respectively. The

344 differences were greater for CMIP6 MME. The highest underestimation by both CMIP  
 345 MMEs was noted in zone C. Both CMIPs MME median and confidence interval band were  
 346 below zero for most of the months. This indicates an underestimation of rainfall by all GCMs  
 347 for both CMIPs in this zone.



348  
 349

Figure 9 Same as Figure 7, but for rainfall

350 Overall, the results support the findings determined in statistical evaluations of the  
 351 models. Table 2 presents the results of the t-test, KS test and F-test for seasonal rainfall,  $T_{mx}$

352 and  $T_{mn}$  of CMIPs seasonal median and ERA5 in different climate zones. Both CMIP5 and  
 353 CMIP6 seasonal MME were statistically indistinguishable at the 95% level based on all three  
 354 tests in all climate zones, except zone Af for the t-test and KS test. The results indicate no  
 355 significant difference in CMIP5 and CMIP6 models in SEA. Inter-model variability of  
 356 CMIP6 GCMs, however, was less than for the CMIP5 GCMs. The uncertainty in simulations  
 357 in CMIP6, therefore, was lower than for the CMIP5 GCMs.

358 Table 2 The results obtained using Student's t-test, KS and F-test for historical seasonal  $T_{mx}$ ,  
 359  $T_{mn}$  and rainfall of CMIP5 and CMIP6 against ERA5 in different climate zones. Zero (0)  
 360 indicates that the test supports the null hypothesis of no difference, while one (1) indicates  
 361 rejection of the null hypothesis at the 5% significance level.

Variable	Month	Zone Af			Zone Am			Zone Aw			Zone C		
		t	KS	F	t	KS	F	t	KS	F	t	KS	F
$T_{mx}$	CMIP5 vs ERA5	1	1	0	0	0	0	0	1	0	0	0	0
	CMIP6 vs ERA5	0	0	0	0	0	0	0	1	0	0	0	0
$T_{mn}$	CMIP5 vs ERA5	1	1	0	0	0	0	0	0	0	0	0	0
	CMIP6 vs ERA5	1	1	0	0	0	0	0	0	0	0	0	0
Rainfall	CMIP5 vs ERA5	0	0	0	0	0	0	0	0	0	0	0	0
	CMIP6 vs ERA5	1	0	0	0	0	0	0	0	0	0	0	0

362

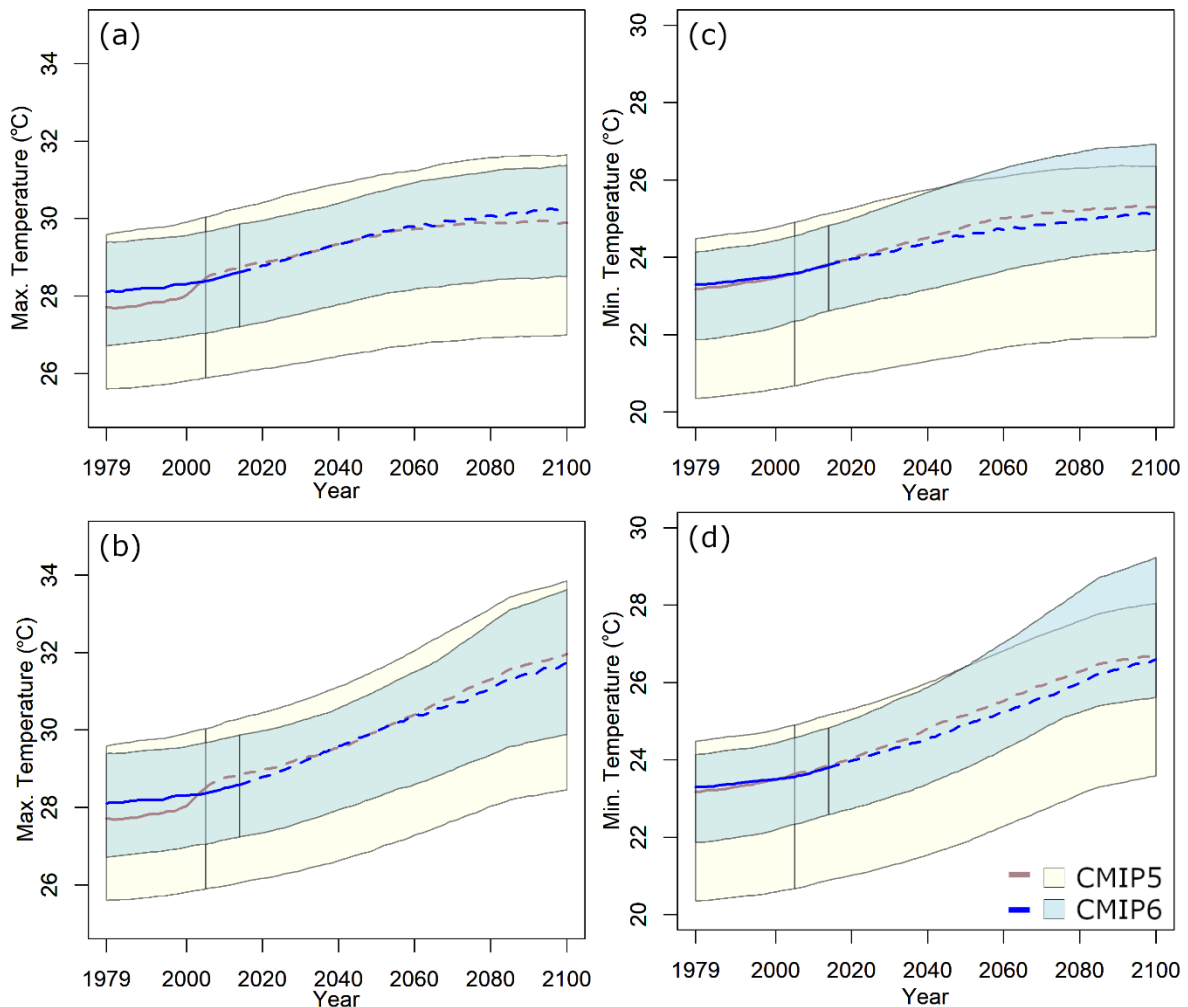
#### 363 4.4. Projected $T_{mx}$ , $T_{mn}$ and rainfall

364 Figure 10 shows the temporal evolution of  $T_{mx}$  (plots a and b) and  $T_{mn}$  (plots c and d) averaged  
 365 over SEA by the MMEs of CMIP5 and CMIP6 for differing scenarios. The upper plots (e.g.,  
 366 a and c) show the projection for medium emission scenarios; RCP4.5 for CMIP5 and SSP2-  
 367 4.5 for CMIP6, respectively, while the lower plots (e.g., b and d) show the projection for  
 368 high-end scenarios; RCP8.5 for CMIP5 and SSP5-8.5 for CMIP6, respectively (Figure 10).  
 369 The MME median projection is presented using an intermediate solid line for the applicable  
 370 historical period (1979 – 2005 for CMIP5 and 1979 – 2014 for CMIP6) and the dashed line  
 371 for the future period, while the band presents the 95% confidence interval of the projections.  
 372 The blue line represents CMIP6, and the brown line represents CMIP5. A 30-year moving  
 373 average is used to smooth the lines.

374 Figure 10 shows a much thinner confidence band (less uncertainty) in the projections  
 375 for CMIP6 than its predecessors, CMIP5. For  $T_{mx}$ , both versions show nearly the same future  
 376 projection for different scenarios for 2020-2059. CMIP6 shows a greater increase in  $T_{mx}$  for  
 377 SSP2-4.5 and a reduced increase for SSP5-8.5 compared to RCP4.5 and 8.5 projections for  
 378 2060-2099.  $T_{mx}$  is projected to reach 30.2 °C and 31.74 °C for SSP2-4.5 and 5-8.5, while  
 379 29.9 °C and 31.97 °C for RCP4.5 and 8.5 by 2100. The CMIP5 MME median shows an

380 abrupt shift in  $T_{mx}$  between the historical estimations and the modeling forecasts. This is not  
 381 seen in the CMIP6 modeling. A gradual increase in  $T_{mx}$  from historical to future periods  
 382 indicates a realistic projection by CMIP6.

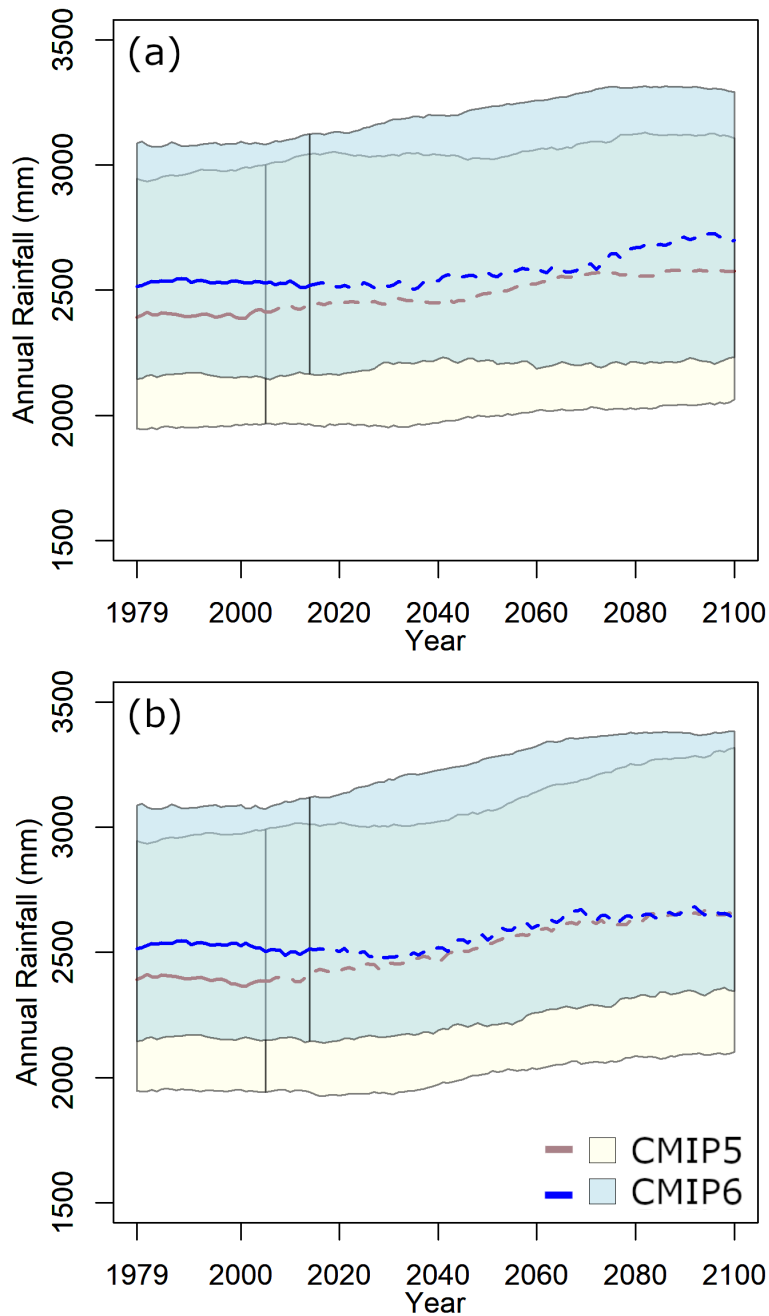
383 The MME median of CMIP6 shows a slight decrease in  $T_{mn}$  in the future (when  
 384 compared to the CMIP5) for both scenarios (Figure 10). The  $T_{mn}$  is projected to reach 25.11  
 385 °C and 26.6 °C for SSP2-4.5 and 5-8.5, and 25.29 °C and 26.7 °C for RCP4.5 and 8.5 by  
 386 2100. As is the case for  $T_{mx}$ , CMIP6 also shows reduced uncertainty in the  $T_{mn}$  projection  
 387 when compared to CMIP5.



388 Figure 10 Temporal evolution of  $T_{mx}$  (°C) (a and b) and  $T_{mn}$  (°C) (c and d) for CMIP5  
 389 (yellow) and CMIP6 (blue) under different scenarios (upper row) RCP4.5 and SSP2-4.5 and  
 390 (lower row) RCP8.5 and SSP5-8.5. Shadings signify 95% projections confidence interval.  
 391 The vertical line indicates the end of the historical estimations.

393

394           Figure 11 shows rainfall projections generated by CMIP5 and CMIP6 MME. The  
395 MME median of CMIP6 indicates the potential for a greater increase in rainfall in the future  
396 than does CMIP5. The uncertainty in the projections of both CMIPs, however, is similar. The  
397 CMIP6 MME projected an increase in rainfall from nearly 2500 mm from the present day to  
398 2700 mm by 2100 for SSP2-4.5, while CMIP5 MME indicated a potential for 2577 mm for  
399 RCP4.5 (Figure 11 (a)). For the higher scenario, the MME of both CMIPs projected the  
400 rainfall to reach 2640 mm by 2100 (Figure 11 (b)). Results indicate a greater decrease in  
401 rainfall for SSP5-8.5 than for SSP2-4.5, and a greater increase in rainfall for RCP8.5 than  
402 RCP4.5.



403

404 Figure 11 Annual rainfall (mm) projection by CMIP5 (yellow) and CMIP6 (blue) models for  
 405 different scenarios: a) medium scenario (RCP4.5 and SSP2-4.5); and b) high scenario  
 406 (RCP8.5 and SSP5-8.5)

407

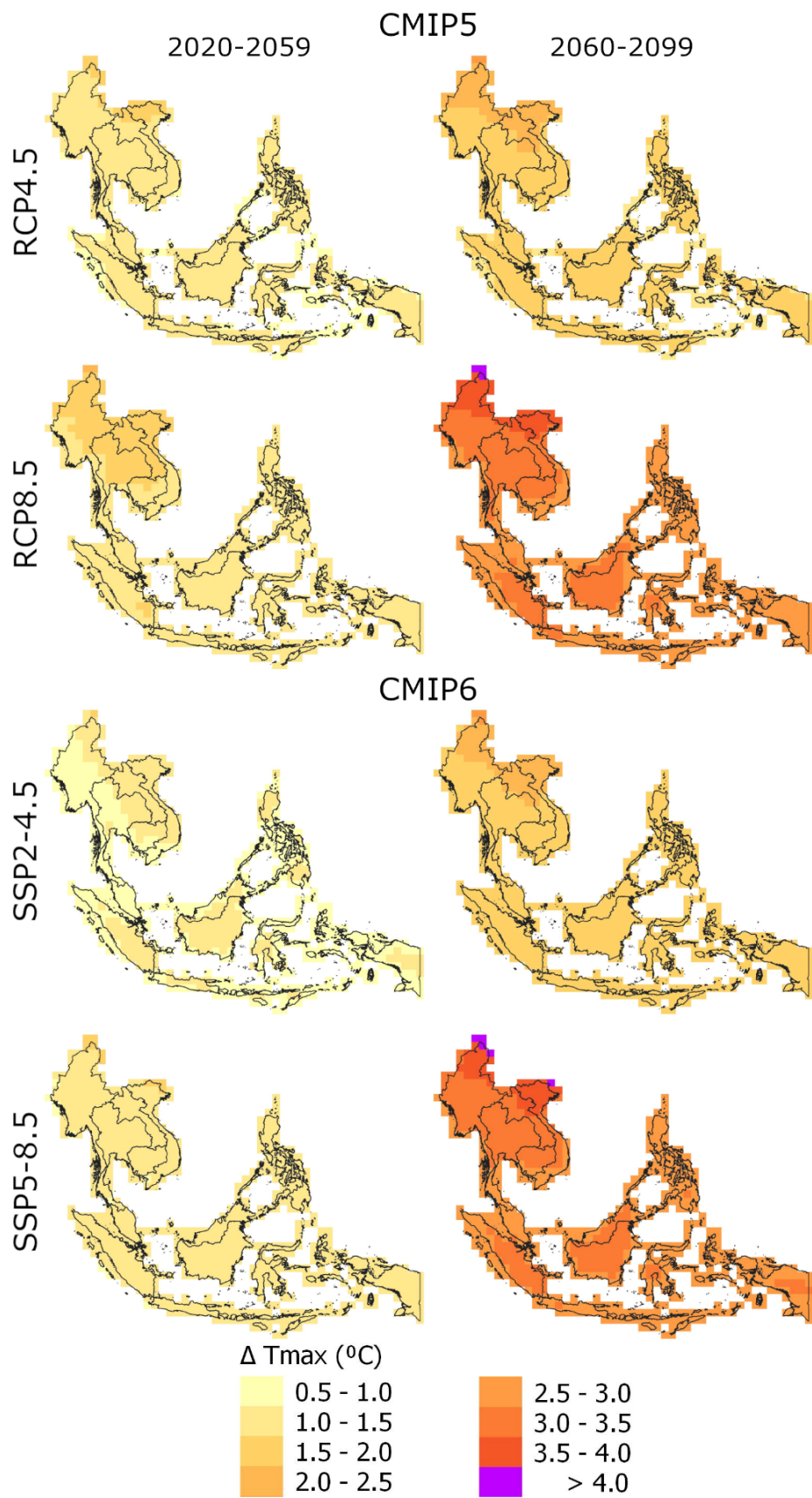
408 **4.5. Spatial changes of temperature and rainfall**

409 Changes in annual  $T_{mx}$ ,  $T_{mn}$  and rainfall were estimated using the MME mean of CMIPs for  
 410 both the near and far futures, and for both the medium and high scenarios. These were  
 411 compared to the historical period (1979-2005).

412 Figure 12 depicts the geographical distribution of projected change ( $^{\circ}\text{C}$ ) in  $T_{\text{mx}}$ . Both  
413 CMIPs projected a rise in  $T_{\text{mx}}$  for the two future periods. However, CMIP6 MME projected  
414 a smaller rise in  $T_{\text{mx}}$  than did CMIP5 MME. The projections of both CMIPs are highly  
415 consistent. Both MMEs projected a maximum increase in  $T_{\text{mx}}$  in the north ( $> 4.0^{\circ}\text{C}$ ), and a  
416 minimum to the southeast (Papua), with a temperature of  $1.0\text{--}1.33^{\circ}\text{C}$  in the near future and  
417  $1.59\text{--}3.01^{\circ}\text{C}$  in far future.  $T_{\text{mx}}$  projections also show a reduced rate of temperature increase  
418 in the central parts of SEA.

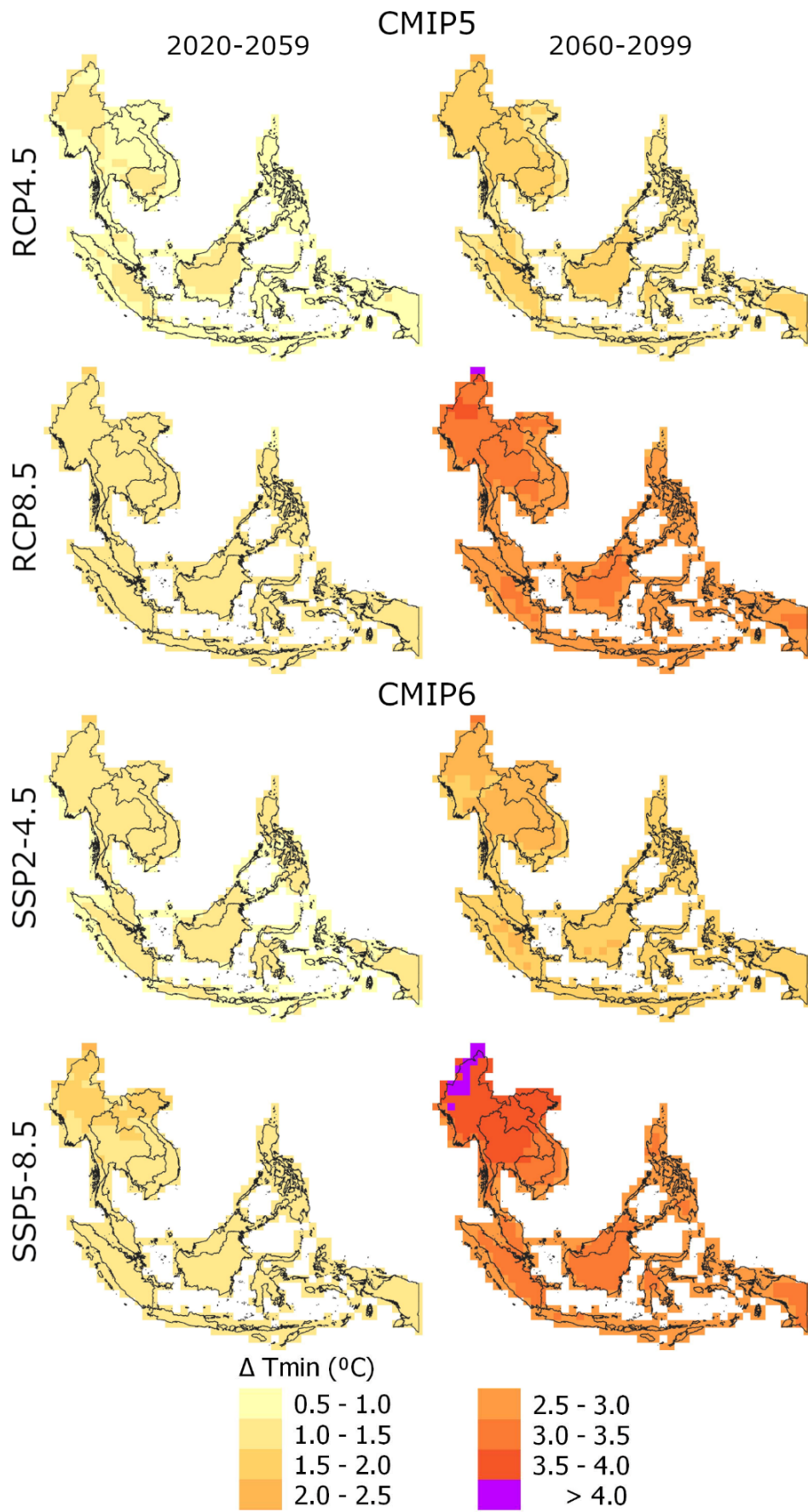
419 The increase in  $T_{\text{mn}}$  was similar to  $T_{\text{mx}}$  (Figure 13). In contrast to  $T_{\text{mx}}$ , however, the  
420 CMIP6 MME modelling projected a greater increase in  $T_{\text{mn}}$  than for CMIP5 MME, for both  
421 projection scenarios in both periods. Overall,  $T_{\text{mn}}$  is projected to increase more than  $T_{\text{mx}}$ . The  
422 greatest increase is seen in the north ( $5.02^{\circ}\text{C}$ ), while the lowest is in the southeast,  $0.96\text{--}1.27$   
423  $^{\circ}\text{C}$  in near future and  $1.57\text{--}3.08^{\circ}\text{C}$  in far future. Both  $T_{\text{mn}}$  and  $T_{\text{mx}}$  show the greatest increase  
424 in regions where historical temperatures are less and vice versa.

425 Figure 14 shows the geographical variability in the projected changes in annual  
426 rainfall in percent. Both the CMIPs MME provided projections for annual rainfall for both  
427 the medium and high scenarios. The greatest increase is projected for the near future for  
428 SSP2-4.5. Both CMIPs, however, display a 25% decrease in rainfall in the south (Java) and  
429 southwest (Sumatra) parts of SEA. Rainfall increases in the northwest (Borneo and  
430 Indonesia) and the southeast (Papua). A 10 to 20% increase in rainfall in those regions is  
431 projected in the far future, for all scenarios. Rainfall would increase in the higher rainfall  
432 regions of SEA.



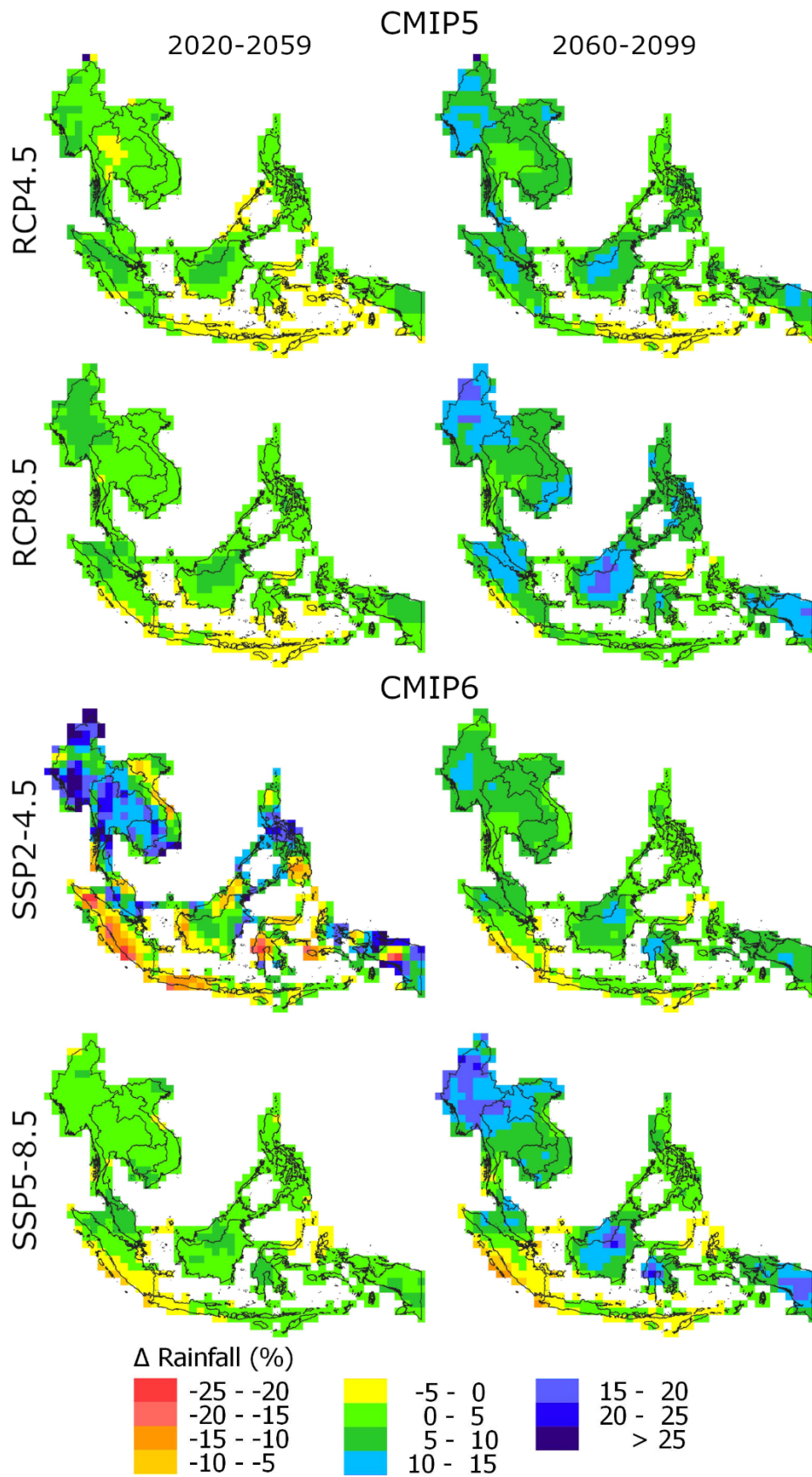
433

434 Figure 12 Geographical variability of the change in  $T_{mx}$  ( $^{\circ}C$ ) over SEA based on MME of  
 435 CMIP5 and CMIP6 for two futures in medium and high projection scenarios



436  
437

Figure 13 Same as Figure 12, but for  $T_{min}$  ( $^{\circ}C$ )



438

439

440

Figure 14 Same as Figure 12, but for rainfall

## 441 **5. Discussion**

442 A large number of studies have examined the ability of CMIP5 and CMIP6 GCMs to estimate  
443 the historical climate in different regions of the globe (Jain et al., 2019; Gusain et al., 2020;  
444 Kamruzzaman et al., 2021; Song et al., 2021a; Yazdandoost et al., 2021). Overall, these  
445 studies have revealed an improvement in the CMIP6 models compared to previous versions,  
446 i.e. CMIP5. Improvements in CMIP6 modelling have been noted in studies of the Tibetan  
447 Plateau (Lun et al., 2021), Central and South America (Ortega et al., 2021), Columbia (Arias  
448 et al., 2021), Mediterranean region (Bağçaci et al., 2021). The superiority of CMIP6 models  
449 over the older CMIP5 models was also reported for extreme indices work over East Africa  
450 (Ayugi et al., 2021), extreme rainfall and temperature in major river basins of China (Zhu et  
451 al., 2021), extreme precipitation over the whole of China (Luo et al., 2021), Australia (Deng  
452 et al., 2021), and Western North Pacific and East Asia (Chen et al., 2021). CMIP6 models  
453 were found to simulate climatic variables more accurately than CMIP5 models. For example,  
454 Jiang et al., (2021) found improved measurement of clouds and vapor over the tropical ocean  
455 using CMIP6. In the nearby region of SEA, Jain et al., (2019) reported enhancement of  
456 CMIP6 GCMs over Central and North India. Gusain et al., (2020) reported the higher  
457 capability of CMIP6 GCMs in estimating the Indian summer rainfall. Song et al., (2021b)  
458 showed an improvement in CMIP6 modelling over South Korea. Kamruzzaman et al., (2021)  
459 found there was an enhanced ability of CMIP6 MME to replicate spatial variability of rainfall  
460 and temperature over Bangladesh when compared with CMIP5 MME.

461 The current study findings were different to those noted in other parts of the world,  
462 with the performance of CMIP6 GCMs found to be similar to that of CMIP5. The KGE  
463 showed an improvement in some of the CMIP6 GCMs in simulating historical rainfall,  
464 however, the Taylor diagram indicated similar performance of GCMs for both CMIPs. The  
465 major difference in the CMIP6 models when compared to the CMIP5 models was less inter-  
466 model variability. Due to this, the uncertainty bond in CMIP6 ensemble was much narrower  
467 than in the CMIP5 ensemble. A comparable finding is reported by Deng et al., (2021) when  
468 comparing the performance of CMIPs in simulating temperature extremes over Australia.  
469 These showed narrower ensemble ranges for CMIP6 models when compared to CMIP5  
470 models (Deng et al., 2021). These results indicate more consistency in simulations using  
471 CMIP6 GCMs when compared to CMIP5 GCMs. All CMIP6 GCMs used the same forcing  
472 datasets and boundary conditions (Taylor et al., 2018). Therefore, the simulations of CMIP6  
473 GCMs are more consistent.

474 The results reported here also contradict the findings from Khadka et al., (2021) over  
475 SEA. That study did not use common models to compare both CMIPs and also used different  
476 subsets of the CMIP5 and CMIP6 GCMs. In the current study, common GCMs for both  
477 CMIPs were used and so provided an estimation of the relative performance of the GCMs.  
478 Khadka et al., (2021) also used correlation and RMSE for measuring the performance of the  
479 GCMs. So two metrics were used to estimate different properties of the model performance.  
480 It should be noted that making decisions using multiple statistical metrics is always  
481 problematic, as using different metrics can often provide different outcomes. For this reason,  
482 the current study used an integrated metric (KGE). This measures the ability of the model to  
483 construct spatial distributions, variables and bias, and thus has provided a reliable assessment  
484 of GCM capability.

485 The SEA is comprised of both mainland and maritime continents. Shallow and deep  
486 marginal seas, with complex land-sea distribution and topography, have resulted in a complex  
487 climatic regime (Robertson et al., 2011). Atmospheric circulation patterns (resulting from the  
488 land-sea configuration) make seasonal temperatures and rainfall asymmetric over the region  
489 (Yoneyama and Zhang, 2020). These factors may have influenced CMIP6 modelling  
490 performance and affected the improved capability noted in other studies when comparing  
491 performance against the older CMIP5 models.

492 This study reported some inconsistencies in the projection of temperature and rainfall  
493 for both the CMIP5 and CMIP6 models. CMIP6 showed a large increase in  $T_{mx}$  for SSP2-4.5  
494 and a small increase for SSP5-8.5, compared to RCP4.5 and 8.5, for the far future projections  
495 (2060-2099). The MME mean of CMIP6 showed a slight decrease in  $T_{mn}$  in future than  
496 CMIP5 for both scenarios. In contrast to  $T_{mx}$ , CMIP6 MME projected an increase in  $T_{mn}$   
497 compared to CMIP5 MME for both projection scenarios in all periods. This has also  
498 contradicted the findings available for other regions. SSP scenarios have previously been  
499 reported as indicating a greater increase in temperature than their equivalent RCP scenarios  
500 (Ortega et al., 2021). However, both CMIPs have reported a greater increase in  $T_{mn}$  when  
501 compared to  $T_{mx}$ , as noted in other regions. The greatest inconsistency in the CMIP5 and  
502 CMIP6 GCMs was in the rainfall projections. The results showed a decrease in rainfall for  
503 SSP5-8.5 as compared to SSP2-4.5, with an increase in rainfall noted for RCP8.5 compared  
504 to RCP4.5. This indicated an increase in rainfall with increase in temperature for CMIP5  
505 MME in the region. In contrast, CMIP6 MME showed a decrease in rainfall for SSP5-8.5  
506 despite a rise in temperature.

507           The spatial distribution of temperature and rainfall changes revealed a greater  
508 increase in temperature in the cooler regions and a reduced increase in the warmer regions.  
509 This was in contrast to the rainfall projections. Increased rainfall was noted in the high rainfall  
510 regions and reduced rainfall in the current low rainfall regions. The results indicated more  
511 homogeneity in the geographical variability of temperature, but more heterogeneity in the  
512 spatial distribution of rainfall. The current temperature in the region is more homogeneous  
513 than in any other part of the world and the present study indicates that this would continue  
514 into the future. In contrast, the current spatial distribution of rainfall in SEA is highly diverse,  
515 ranging from 750 mm to >6000 mm. Some parts of Papua in the southeast receive the highest  
516 rainfall globally (~ 11000 mm). The SEA has the highest density of animal life on the planet  
517 with the various species inhabiting a narrow climatic niche. Climate change is expected to  
518 increase species diversity.

519

## 520 **6. Conclusion**

521 The present study evaluated the use of CMIP5 and CMIP6 in developing present and future  
522 climate projections for the Southeast Asia region. Uncertainties in historical simulation and  
523 future projections of the CMIPs were also examined as part of determining overall model  
524 performance. The study revealed no significant improvement in GCMs (from CMIP5 to  
525 CMIP6) in simulating present-day temperature and rainfall over SEA. However, the CMIP6  
526 ensemble did display less uncertainty in the simulation work than CMIP5. This indicated a  
527 greater degree of confidence could be assumed in any decision-making based on the CMIP6  
528 projections. Both CMIPs revealed that a rise in temperature and rainfall in most of SEA  
529 would occur. Some inconsistencies in the CMIP5 and CMIP6 models projections were noted.  
530 This has emphasized the need to streamline existing adaptation measures, particularly those  
531 arising from CMIP6 SSP scenarios. The study projected a decrease or an insignificant  
532 increase in rainfall in the low rainfall region. This may increase both flood and water stress  
533 in the region. Any changes in the homogeneity in temperature and rainfall could significantly  
534 affect the biodiversity in the region. Future modelling should take account of the increased  
535 availability of GCMs both CMIPs, and utilize the ability to compare and contrast the various  
536 model iterations.

537

538 **Declarations**

539 **Funding**

540 The authors are grateful to Staffordshire University, UK for providing financial support for  
541 this research through grant no. WR GCRF 2020-2021. Authors are also grateful to the Belt  
542 and Road Special Foundation of the State Key Laboratory of Hydrology-Water Resources  
543 and Hydraulic Engineering to support this research through grants no. (2019491311 &  
544 2020491011).

545 **Conflicts of interest/Competing interests**

546 The authors declare that they have no known competing financial interests or personal  
547 relationships that could have appeared to influence the work reported in this paper.

548 **Code availability**

549 The code was written using R software, R.3.4, to produce the data. The code is available upon  
550 request.

551 **Author contributions**

552 All authors contributed to the study conception and design.

553

## References

- 554 Alvares, C.A., Stape, J.L., Sentelhas, P.C., De Moraes Gonçalves, J.L., Sparovek, G., 2013.  
555 Köppen's climate classification map for Brazil. *Meteorol. Zeitschrift* 22, 711–728.  
556 <https://doi.org/10.1127/0941-2948/2013/0507>
- 557 Arias, P.A., Ortega, G., Villegas, L.D., Martínez, J.A., 2021. Colombian climatology in  
558 CMIP5/CMIP6 models: Persistent biases and improvements . *Rev. Fac. Ing. Univ.*  
559 *Antioquia* .
- 560 Ayugi, B., Jiang, Z., Zhu, H., Ngoma, H., Babaousmail, H., Karim, R., Dike, V., 2021.  
561 Comparison of CMIP6 and CMIP5 models in simulating mean and extreme  
562 precipitation over East Africa. *Int. J. Climatol.* n/a. <https://doi.org/10.1002/joc.7207>
- 563 Bağçacı, S.Ç., Yucel, I., Duzenli, E., Yilmaz, M.T., 2021. Intercomparison of the expected  
564 change in the temperature and the precipitation retrieved from CMIP6 and CMIP5  
565 climate projections: A Mediterranean hot spot case, Turkey. *Atmos. Res.* 256, 105576.  
566 <https://doi.org/10.1016/j.atmosres.2021.105576>
- 567 Baker, N.C., Huang, H.P., 2014. A comparative study of precipitation and evaporation  
568 between CMIP3 and CMIP5 climate model ensembles in semiarid regions. *J. Clim.* 27,  
569 3731–3749. <https://doi.org/10.1175/JCLI-D-13-00398.1>
- 570 Bourdeau-Goulet, S.C., Hassanzadeh, E., 2021. Comparisons Between CMIP5 and CMIP6  
571 Models: Simulations of Climate Indices Influencing Food Security, Infrastructure  
572 Resilience, and Human Health in Canada. *Earth's Futur.* 9, 1–17.  
573 <https://doi.org/10.1029/2021EF001995>
- 574 Chang, C.P., Zhuo, W., John, M., Ching-Hwang, L., 2005. Annual Cycle of Southeast  
575 Asia—Maritime Continent Rainfall and the Asymmetric Monsoon Transition. *J. Clim.*  
576 18, 287–301. <https://doi.org/10.1175/JCLI-3257.1>
- 577 Chen, C.-A., Hsu, H.-H., Liang, H.-C., 2021. Evaluation and comparison of CMIP6 and  
578 CMIP5 model performance in simulating the seasonal extreme precipitation in the  
579 Western North Pacific and East Asia. *Weather Clim. Extrem.* 31, 100303.  
580 <https://doi.org/10.1016/j.wace.2021.100303>
- 581 Chen, H., Sun, J., Chen, X., 2014. Projection and uncertainty analysis of global  
582 precipitation-related extremes using CMIP5 models. *Int. J. Climatol.* 34, 2730–2748.  
583 <https://doi.org/10.1002/joc.3871>
- 584 Deng, X., Perkins-Kirkpatrick, S.E., Lewis, S.C., Ritchie, E.A., 2021. Evaluation of  
585 Extreme Temperatures Over Australia in the Historical Simulations of CMIP5 and  
586 CMIP6 Models. *Earth's Futur.* 9, e2020EF001902.  
587 <https://doi.org/10.1029/2020EF001902>
- 588 Desmet, Q., Ngo-Duc, T., 2021. A novel method for ranking CMIP6 global climate models  
589 over the southeast Asian region. *Int. J. Climatol.* 1–21.  
590 <https://doi.org/10.1002/joc.7234>
- 591 Dewi, R.G., 2010. Indonesia second national communication under the United Nations  
592 Framework Convention on Climate Change (UNFCCC). Ministry of Environment,  
593 Republic of Indonesia.
- 594 Eyring, V., Bony, S., Meehl, G.A., Senior, C.A., Stevens, B., Stouffer, R.J., Taylor, K.E.,  
595 2016. Overview of the Coupled Model Intercomparison Project Phase 6 (CMIP6)

- 596 experimental design and organization. *Geosci. Model Dev.* 9, 1937–1958.  
597 <https://doi.org/10.5194/gmd-9-1937-2016>
- 598 Flato, G., Marotzke, J., Abiodun, B., Braconnot, P., Chou, S.C., Collins, W., Cox, P.,  
599 Driouech, F., Emori, S., Eyring, V., 2013. Climate change 2013: the physical science  
600 basis. contribution of working group I to the fifth assessment report of the  
601 intergovernmental panel on climate change. *Eval. Clim. Model.* eds TF Stock. D. Qin,  
602 G.-K. Plattner, M. Tignor, SK Allen, J. Boschung, al.(Cambridge Cambridge Univ.  
603 Press.
- 604 Gao, J., Sheshukov, A.Y., Yen, H., Douglas-Mankin, K.R., White, M.J., Arnold, J.G.,  
605 2019. Uncertainty of hydrologic processes caused by bias-corrected CMIP5 climate  
606 change projections with alternative historical data sources. *J. Hydrol.* 568, 551–561.  
607 <https://doi.org/https://doi.org/10.1016/j.jhydrol.2018.10.041>
- 608 Ge, F., Zhu, S., Peng, T., Zhao, Y., Sielmann, F., Fraedrich, K., Zhi, X., Liu, X., Tang, W.,  
609 Ji, L., 2019. Risks of precipitation extremes over Southeast Asia: Does 1.5 °C or 2 °C  
610 global warming make a difference? *Environ. Res. Lett.* 14.  
611 <https://doi.org/10.1088/1748-9326/aaff7e>
- 612 Gupta, H. V., Kling, H., Yilmaz, K.K., Martinez, G.F., 2009. Decomposition of the mean  
613 squared error and NSE performance criteria: Implications for improving hydrological  
614 modelling. *J. Hydrol.* 377, 80–91. <https://doi.org/10.1016/j.jhydrol.2009.08.003>
- 615 Gusain, A., Ghosh, S., Karmakar, S., 2020. Added value of CMIP6 over CMIP5 models in  
616 simulating Indian summer monsoon rainfall. *Atmos. Res.* 232, 104680.  
617 <https://doi.org/10.1016/j.atmosres.2019.104680>
- 618 Hamed, M.M., Nashwan, M.S., Shahid, S., 2021a. Intercomparison of Historical Simulation  
619 and Future Projection of Rainfall and Temperature by CMIP5 and CMIP6 GCMs Over  
620 Egypt.
- 621 Hamed, M.M., Nashwan, M.S., Shahid, S., 2021b. Performance Evaluation of Reanalysis  
622 Precipitation Products in Egypt using Fuzzy Entropy Time Series Similarity Analysis.  
623 *Int. J. Climatol.* 41, 5431– 5446. <https://doi.org/10.1002/joc.7286>
- 624 Hartmann, D.L., 2016. Chapter 11 - Global Climate Models, in: Hartmann, D.L.B.T.-  
625 G.P.C. (Second E. (Ed.), . Elsevier, Boston, pp. 325–360.  
626 <https://doi.org/10.1016/B978-0-12-328531-7.00011-6>
- 627 Hersbach, H., Bell, B., Berrisford, P., Hirahara, S., Horányi, A., Muñoz-Sabater, J.,  
628 Nicolas, J., Peubey, C., Radu, R., Schepers, D., Simmons, A., Soci, C., Abdalla, S.,  
629 Abellan, X., Balsamo, G., Bechtold, P., Biavati, G., Bidlot, J., Bonavita, M., De  
630 Chiara, G., Dahlgren, P., Dee, D., Diamantakis, M., Dragani, R., Flemming, J., Forbes,  
631 R., Fuentes, M., Geer, A., Haimberger, L., Healy, S., Hogan, R.J., Hólm, E.,  
632 Janisková, M., Keeley, S., Laloyaux, P., Lopez, P., Lupu, C., Radnoti, G., de Rosnay,  
633 P., Rozum, I., Vamborg, F., Villaume, S., Thépaut, J.-N., 2020. The ERA5 global  
634 reanalysis. *Q. J. R. Meteorol. Soc.* 146, 1999–2049. <https://doi.org/10.1002/qj.3803>
- 635 IPCC, 2007. Climate change 2007-the physical science basis: Working group I contribution  
636 to the fourth assessment report of the IPCC.
- 637 Iqbal, Z., Shahid, S., Ahmed, K., Ismail, T., Ziarh, G.F., Chung, E.-S., Wang, X., 2021.  
638 Evaluation of CMIP6 GCM rainfall in mainland Southeast Asia. *Atmos. Res.* 254,  
639 105525. <https://doi.org/10.1016/j.atmosres.2021.105525>

- 640 Jain, S., Salunke, P., Mishra, S.K., 2019. Advantage of NEX-GDDP over CMIP5 and  
641 CORDEX data: Indian summer monsoon. *Atmos Res* 228.  
642 <https://doi.org/10.1016/j.atmosres.2019.05.026>
- 643 Jiang, J.H., Su, H., Wu, L., Zhai, C., Schiro, K.A., 2021. Improvements in Cloud and Water  
644 Vapor Simulations Over the Tropical Oceans in CMIP6 Compared to CMIP5. *Earth*  
645 *Sp. Sci.* 8, e2020EA001520. <https://doi.org/https://doi.org/10.1029/2020EA001520>
- 646 Kamruzzaman, M., Shahid, S., Islam, A.R.M.T., Hwang, S., Cho, J., Zaman, M.A.U.,  
647 Ahmed, M., Rahman, M.M., Hossain, M.B., 2021. Comparison of CMIP6 and CMIP5  
648 Model Performance in Simulating Historical Precipitation and Temperature in  
649 Bangladesh: A Preliminary Study. *Theor. Appl. Climatol.* 145, 1385–1406.
- 650 Kang, S., Im, E.S., Eltahir, E.A.B., 2019. Future climate change enhances rainfall  
651 seasonality in a regional model of western Maritime Continent. *Clim. Dyn.* 52, 747–  
652 764. <https://doi.org/10.1007/s00382-018-4164-9>
- 653 Khadka, D., Babel, M.S., Abatan, A.A., Collins, M., 2021. An Evaluation of CMIP5 and  
654 CMIP6 Climate Models in Simulating Summer Rainfall in the Southeast Asian  
655 Monsoon Domain. *Int. J. Climatol.* n/a. <https://doi.org/10.1002/joc.7296>
- 656 Khan, N., Pour, S.H., Shahid, S., Ismail, T., Ahmed, K., Chung, E.S., Nawaz, N., Wang, X.,  
657 2019. Spatial distribution of secular trends in rainfall indices of Peninsular Malaysia in  
658 the presence of long-term persistence. *Meteorol. Appl.* 26, 655–670.  
659 <https://doi.org/10.1002/met.1792>
- 660 Kling, H., Fuchs, M., Paulin, M., 2012. Runoff conditions in the upper Danube basin under  
661 an ensemble of climate change scenarios. *J. Hydrol.* 424–425, 264–277.  
662 <https://doi.org/10.1016/j.jhydrol.2012.01.011>
- 663 Knoben, W.J.M., Freer, J.E., Woods, R.A., 2019. Technical note: Inherent benchmark or  
664 not? Comparing Nash-Sutcliffe and Kling-Gupta efficiency scores. *Hydrol. Earth Syst.*  
665 *Sci. Discuss.* 1–7. <https://doi.org/10.5194/hess-2019-327>
- 666 Lee, H.M., Yoo, D.G., Kim, J.H., Kang, D., Min, L.H., Guen, Y. Do, Hoon, K.J., Doosun,  
667 K., 2017. Hydraulic Simulation Techniques for Water Distribution Networks to Treat  
668 Pressure Deficient Conditions. *J. Water Resour. Plan. Manag.* 144, 07017008.  
669 [https://doi.org/10.1061/\(asce\)wr.1943-5452.0000899](https://doi.org/10.1061/(asce)wr.1943-5452.0000899)
- 670 Li, X.-X., 2020. Heat wave trends in Southeast Asia during 1979–2018: The impact of  
671 humidity. *Sci. Total Environ.* 721. <https://doi.org/10.1016/j.scitotenv.2020.137664>
- 672 Lun, Y., Liu, L., Cheng, L., Li, X., Li, H., Xu, Z., 2021. Assessment of GCMs simulation  
673 performance for precipitation and temperature from CMIP5 to CMIP6 over the  
674 Tibetan Plateau. *Int. J. Climatol.* 41, 3994–4018.  
675 <https://doi.org/https://doi.org/10.1002/joc.7055>
- 676 Luo, N., Guo, Y., Chou, J., Gao, Z., 2021. Added value of CMIP6 models over CMIP5  
677 models in simulating the climatological precipitation extremes in China. *Int. J.*  
678 *Climatol.* n/a. <https://doi.org/https://doi.org/10.1002/joc.7294>
- 679 McSweeney, C.F., Jones, R.G., Lee, R.W., Rowell, D.P., 2015. Selecting CMIP5 GCMs for  
680 downscaling over multiple regions. *Clim. Dyn.* 44, 3237–3260.  
681 <https://doi.org/10.1007/s00382-014-2418-8>
- 682 Moss, R.H., Edmonds, J.A., Hibbard, K.A., Manning, M.R., Rose, S.K., van Vuuren, D.P.,

683 Carter, T.R., Emori, S., Kainuma, M., Kram, T., Meehl, G.A., Mitchell, J.F.B.,  
684 Nakicenovic, N., Riahi, K., Smith, S.J., Stouffer, R.J., Thomson, A.M., Weyant, J.P.,  
685 Wilbanks, T.J., 2010. The next generation of scenarios for climate change research and  
686 assessment. *Nature* 463, 747–756. <https://doi.org/10.1038/nature08823>

687 Muhammad, M.K.I., Nashwan, M.S., Shahid, S., Ismail, T. bin, Song, Y.H., Chung, E.S.,  
688 2019. Evaluation of empirical reference evapotranspiration models using compromise  
689 programming: A case study of Peninsular Malaysia. *Sustain.* 11.  
690 <https://doi.org/10.3390/su11164267>

691 Nashwan, M.S., Ismail, T., Ahmed, K., 2018a. Flood susceptibility assessment in Kelantan  
692 river basin using copula. *Int. J. Eng. Technol.* 7, 584–590.  
693 <https://doi.org/10.14419/ijet.v7i2.8876>

694 Nashwan, M.S., Shahid, S., 2022. Future precipitation changes in Egypt under the 1.5 and  
695 2.0°C global warming goals using CMIP6 multimodel ensemble. *Atmos. Res.* 265,  
696 105908. <https://doi.org/https://doi.org/10.1016/j.atmosres.2021.105908>

697 Nashwan, M.S., Shahid, S., Chung, E.S., Ahmed, K., Song, Y.H., 2018b. Development of  
698 climate-based index for hydrologic hazard susceptibility. *Sustain.* 10.  
699 <https://doi.org/10.3390/su10072182>

700 Nasional, B.P.P., 2012. National Action Plan for Climate Change Adaptation (RAN-API),  
701 Jakarta: Bappenas.

702 Neale, R., Slingo, J., 2003. The Maritime Continent and its role in the global climate: A  
703 GCM study. *J. Clim.* 16, 834–848. [https://doi.org/10.1175/1520-0442\(2003\)016<0834:TMCAIR>2.0.CO;2](https://doi.org/10.1175/1520-0442(2003)016<0834:TMCAIR>2.0.CO;2)

705 Noor, M., Ismail, T., Shahid, S., Nashwan, M.S., Ullah, S., 2019. Development of multi-  
706 model ensemble for projection of extreme rainfall events in Peninsular Malaysia.  
707 *Hydrol. Res.* 50, 1772–1788. <https://doi.org/10.2166/nh.2019.097>

708 Ortega, G., Arias, P.A., Villegas, J.C., Marquet, P.A., Nobre, P., 2021. Present-day and  
709 future climate over central and South America according to CMIP5/CMIP6 models.  
710 *Int. J. Climatol.* n/a. <https://doi.org/https://doi.org/10.1002/joc.7221>

711 Peel, M.C., Finlayson, B.L., McMahon, T.A., 2007. Updated world map of the Köppen-  
712 Geiger climate classificatio. *Hydrol. Earth Syst. Sci.* 11, 1633–1644.  
713 <https://doi.org/10.1002/ppp.421>

714 Qian, J.H., 2008. Why precipitation is mostly concentrated over islands in the maritime  
715 continent. *J. Atmos. Sci.* 65, 1428–1441. <https://doi.org/10.1175/2007JAS2422.1>

716 Radcliffe, D.E., Mukundan, R., 2017. PRISM vs. CFSR Precipitation Data Effects on  
717 Calibration and Validation of SWAT Models. *J. Am. Water Resour. Assoc.* 53, 89–  
718 100. <https://doi.org/10.1111/1752-1688.12484>

719 Raghavan, S. V., Vu, M.T., Liong, S.Y., 2017. Ensemble climate projections of mean and  
720 extreme rainfall over Vietnam. *Glob. Planet. Change* 148, 96–104.  
721 <https://doi.org/10.1016/j.gloplacha.2016.12.003>

722 ROBERTSON, A.W., MORON, V., QIAN, J.-H., CHANG, C.-P., TANGANG, F.,  
723 ALDRIAN, E., KOH, T.Y., LIEW, J., 2011. THE MARITIME CONTINENT  
724 MONSOON, in: *The Global Monsoon System, World Scientific Series on Asia-  
725 Pacific Weather and Climate. WORLD SCIENTIFIC*, pp. 85–98.

- 726 [https://doi.org/doi:10.1142/9789814343411\\_0006](https://doi.org/doi:10.1142/9789814343411_0006)
- 727 Salman, S.A., Nashwan, M.S., Ismail, T., Shahid, S., 2020. Selection of CMIP5 general  
728 circulation model outputs of precipitation for peninsular Malaysia. *Hydrol. Res.* 51,  
729 781–798. <https://doi.org/10.2166/nh.2020.154>
- 730 Sardeshmukh, P.D., Compo, G.P., Penland, C., 2000. Changes of Probability Associated  
731 with El Nino. *J. Clim.* 13, 4268–4286.
- 732 Schlund, M., Lauer, A., Gentine, P., Sherwood, S.C., Eyring, V., 2020. Emergent  
733 constraints on Equilibrium Climate Sensitivity in CMIP5 : do they hold for CMIP6 ?  
734 *Earth Syst. Dyn.* 1–40. <https://doi.org/10.5194/esd-2020-49>
- 735 Shahid, S., 2010. Probable impacts of climate change on public health in Bangladesh. *Asia-  
736 Pacific J. public Heal.* 22, 310–319. <https://doi.org/10.1177/1010539509335499>
- 737 Shahid, S., Pour, S.H., Wang, X., Shourav, S.A., Minhans, A., Ismail, T. bin, 2017. Impacts  
738 and adaptation to climate change in Malaysian real estate. *Int. J. Clim. Chang. Strateg.  
739 Manag.* 9, 87–103. <https://doi.org/10.1108/IJCCSM-01-2016-0001>
- 740 Song, Y.H., Chung, E.-S., Shahid, S., 2021a. Spatiotemporal differences and uncertainties  
741 in projections of precipitation and temperature in South Korea from CMIP6 and  
742 CMIP5 general circulation models. *Int. J. Climatol.* n/a.  
743 <https://doi.org/10.1002/joc.7159>
- 744 Song, Y.H., Nashwan, M.S., Chung, E.S., Shahid, S., 2021b. Advances in CMIP6 INM-  
745 CM5 over CMIP5 INM-CM4 for precipitation simulation in South Korea. *Atmos. Res.*  
746 247, 105261. <https://doi.org/10.1016/j.atmosres.2020.105261>
- 747 Sperber, K.R., Annamalai, H., Kang, I.-S., Kitoh, A., Moise, A., Turner, A., Wang, B.,  
748 Zhou, T., 2013. The Asian summer monsoon: an intercomparison of CMIP5 vs.  
749 CMIP3 simulations of the late 20th century. *Clim. Dyn.* 41, 2711–2744.  
750 <https://doi.org/10.1007/s00382-012-1607-6>
- 751 Supari, Tangang, F., Juneng, L., Cruz, F., Chung, J.X., Ngai, S.T., Salimun, E., Mohd,  
752 M.S.F., Santisirisomboon, J., Singhruck, P., PhanVan, T., Ngo-Duc, T., Narisma, G.,  
753 Aldrian, E., Gunawan, D., Sopaheluwakan, A., 2020. Multi-model projections of  
754 precipitation extremes in Southeast Asia based on CORDEX-Southeast Asia  
755 simulations. *Environ. Res.* 184, 109350. <https://doi.org/10.1016/j.envres.2020.109350>
- 756 Supharatid, S., Nafung, J., Aribarg, T., 2021. Projected changes in temperature and  
757 precipitation over mainland Southeast Asia by CMIP6 models. *J. Water Clim. Chang.*  
758 1–20. <https://doi.org/10.2166/wcc.2021.015>
- 759 Tangang, F., Chung, J.X., Juneng, L., Supari, Salimun, E., Ngai, S.T., Jamaluddin, A.F.,  
760 Mohd, M.S.F., Cruz, F., Narisma, G., Santisirisomboon, J., Ngo-Duc, T., Van Tan, P.,  
761 Singhruck, P., Gunawan, D., Aldrian, E., Sopaheluwakan, A., Grigory, N., Remedio,  
762 A.R.C., Sein, D. V., Hein-Griggs, D., McGregor, J.L., Yang, H., Sasaki, H., Kumar,  
763 P., 2020. Projected future changes in rainfall in Southeast Asia based on CORDEX–  
764 SEA multi-model simulations. *Clim. Dyn.* 55, 1247–1267.  
765 <https://doi.org/10.1007/s00382-020-05322-2>
- 766 Taylor, K.E., 2001. Summarizing multiple aspects of model performance in a single  
767 diagram. *J. Geophys. Res. Atmos.* 106, 7183–7192.  
768 <https://doi.org/10.1029/2000JD900719>

- 769 Taylor, K.E., Balaji, V., Hankin, S., Juckes, M., Lawrence, B., Pascoe, S., 2011. CMIP5  
770 data reference syntax (DRS) and controlled vocabularies. San Francisco Bay Area,  
771 CA, USA.
- 772 Taylor, K.E., Stouffer, R.J., Meehl, G.A., 2012. An overview of CMIP5 and the experiment  
773 design. *Bull. Am. Meteorol. Soc.* 93, 485–498. [https://doi.org/10.1175/BAMS-D-11-](https://doi.org/10.1175/BAMS-D-11-00094.1)  
774 [00094.1](https://doi.org/10.1175/BAMS-D-11-00094.1)
- 775 Taylor, M.A., Clarke, L.A., Centella, A., Bezanilla, A., Stephenson, T.S., Jones, J.J.,  
776 Campbell, J.D., Vichot, A., Charlery, J., 2018. Future Caribbean climates in a world of  
777 rising temperatures: The 1.5 vs 2.0 dilemma. *J. Clim.* 31, 2907–2926.  
778 <https://doi.org/10.1175/JCLI-D-17-0074.1>
- 779 Thirumalai, K., DiNezio, P.N., Okumura, Y., Deser, C., 2017. Extreme temperatures in  
780 Southeast Asia caused by El Niño and worsened by global warming. *Nat. Commun.* 8,  
781 15531. <https://doi.org/10.1038/ncomms15531>
- 782 van Vuuren, D.P., Edmonds, J., Kainuma, M., Riahi, K., Thomson, A., Hibbard, K., Hurtt,  
783 G.C., Kram, T., Krey, V., Lamarque, J.-F., Masui, T., Meinshausen, M., Nakicenovic,  
784 N., Smith, S.J., Rose, S.K., 2011. The representative concentration pathways: an  
785 overview. *Clim. Change* 109, 5. <https://doi.org/10.1007/s10584-011-0148-z>
- 786 Weigel, A.P., Knutti, R., Liniger, M.A., Appenzeller, C., 2010. Risks of model weighting in  
787 multimodel climate projections. *J. Clim.* 23, 4175–4191.  
788 <https://doi.org/10.1175/2010JCLI3594.1>
- 789 Yang, S., Wu, R., Jian, M., Huang, J., Hu, X., Wang, Z., Jiang, X., 2021. *Climate Change*  
790 *in Southeast Asia and Surrounding Areas*. Springer Climate.
- 791 Yazdandoost, F., Moradian, S., Izadi, A., Aghakouchak, A., 2021. Evaluation of CMIP6  
792 precipitation simulations across different climatic zones: Uncertainty and model  
793 intercomparison. *Atmos. Res.* 250, 105369.  
794 <https://doi.org/10.1016/j.atmosres.2020.105369>
- 795 Yoneyama, K., Zhang, C., 2020. Years of the Maritime Continent. *Geophys. Res. Lett.* 47,  
796 e2020GL087182. <https://doi.org/https://doi.org/10.1029/2020GL087182>
- 797 Zhai, J., Mondal, S.K., Fischer, T., Wang, Y., Su, B., Huang, J., Tao, H., Wang, G., Ullah,  
798 W., Uddin, M.J., 2020. Future drought characteristics through a multi-model ensemble  
799 from CMIP6 over South Asia. *Atmos. Res.* 246, 105111.  
800 <https://doi.org/10.1016/j.atmosres.2020.105111>
- 801 Zhu, X., Lee, S.-Y., Wen, X., Ji, Z., Lin, L., Wei, Z., Zheng, Z., Xu, D., Dong, W., 2021.  
802 Extreme climate changes over three major river basins in China as seen in CMIP5 and  
803 CMIP6. *Clim. Dyn.* <https://doi.org/10.1007/s00382-021-05767-z>
- 804 Ziarh, G.F., Asaduzzaman, M., Dewan, A., Nashwan, M.S., Shahid, S., 2021. Integration of  
805 catastrophe and entropy theories for flood risk mapping in peninsular Malaysia. *J.*  
806 *Flood Risk Manag.* 14, e12686. <https://doi.org/https://doi.org/10.1111/jfr3.12686>
- 807 Zuluaga, C.F., Avila-Diaz, A., Justino, F.B., Wilson, A.B., 2021. Climatology and trends of  
808 downward shortwave radiation over Brazil. *Atmos. Res.* 250, 105347.  
809 <https://doi.org/10.1016/j.atmosres.2020.105347>

810